EVALUATING THE EFFECTS OF SOIL AND ENVIRONMENTAL CONDITIONS FOR SOIL-GAS RADON TESTING PRIOR TO CONSTRUCTION

By

E. SALIMI TARI

A DISSERTATION PRESENTED TO THE GRADUATE SCHOOL
OF THE UNIVERSITY OF FLORIDA IN PARTIAL FULFILLMENT
OF THE REQUIREMENTS FOR THE DEGREE OF
DOCTOR OF PHILOSOPHY

UNIVERSITY OF FLORIDA

1999

ACKNOWLEDGMENTS

I would like to express my sincere thanks and appreciation to the members of the supervisory committee and to all the people who participated in one way or another during the course of this research.

In particular, I would like to extend special thanks to Dr. Fazil Najafi, the chairman of my supervisory committee, for his guidance, encouragement, and patience. Special thanks are extended to the committee members: Dr. M. Tia with the Department of Civil Engineering, Dr. Samim Anghaie with the Department of Nuclear and Radiological Engineering, Dr. Roy Bolduck with the College of Education, and Dr. Kaiss Al-Ahmady with Conley, Rose & Tayon, for their discussions, advice, and review of the final manuscript of this dissertation. I am grateful for the instrumental assistance provided by Dr. Al-Ahmady. His deep knowledge of the subject of this research and his continual assistance made this work possible.

Partial support for this research was provided by the Florida Department of Community Affairs, as part of the Florida Radon Research Program. This support is respectfully acknowledged.

Finally, I would like to express my appreciation and thanks to my wife, Pouran, and my daughter, Maryam, whose patience, understanding, and moral support were always available and were needed to accomplish my research. I also deeply appreciate my father, Shokrolah, and my mother, Pari, for all the support they have given in my life.

TABLE OF CONTENTS

page

ACKNOWLEDGMENTS..... ii

LIST OF TABLES..... vi

LIST OF FIGURES.....viii

ABSTRACT.....xiii

CHAPTERS

1 INTRODUCTION AND LITERATURE SURVEY..... 1

Statement of the Problem..... 1
Objectives of the Research..... 3
Properties of Radon..... 4
Health Hazards of Indoor Radon Exposure..... 6
Availability of Radon in the Soil Gas..... 10
Radon Transport in Soils..... 22

2 METHODOLOGY AND EXPERIMENTAL DESIGN..... 36

Scope of the Methodology..... 36

Soil-Gas Radon Testing Methodology..... 39
Design of the Testing Chamber..... 41
Design of the Experimental Procedure..... 43
Design of Pressure Measurements..... 46
Design of Temperature and Humidity Measurements..... 48
Design of Data Collection..... 50
Design of Soil-Gas Radon Measurements..... 51
Collection and Processing of the Experimental Raw Data..... 54
Design of Tube-Length Effect Experiments..... 56
Quality Control and Assurance..... 58

3 RESULTS AND DISCUSSION..... 65

Observations and Evaluation of the Testing Configuration Condition..... 65
Observations and Evaluation of the Temperature Condition..... 83
Evaluation of the Soil Compaction Condition..... 91
Observations and Evaluation of the Soil Moisture Condition..... 103
The Construction-Management Approach..... 129

4 SUMMARY AND CONCLUSIONS.....137

REFERENCES..... 149

BIOGRAPHICAL SKETCH..... 155

LIST OF TABLES

Table No.		page
1-1	Selected physical properties of radon.....	7
1-2	Major characteristics of ^{222}Rn and its decay products (part of ^{238}U decay chain).....	7
1-3	The risk of exposure to annual radon levels.....	10
1-4	Possible number of lung cancers and comparison of the risk of radon exposure for smokers.....	12
1-5	Possible number of lung cancers and comparison of the risk of radon exposure for nonsmokers.....	13
3-1	Results of the tubing length (5, 10, and 15 feet) effect on the measured radon concentration using the testing setup of Figure 3-6.....	67
3-2	Results of the tubing length (20, 25, and 30 feet) effect on the measured radon concentration using the testing setup of Figure 3-6.....	69
3-3	Results of the tubing length (35, 40, and 45 feet) effect on the measured radon concentration using the testing setup of Figure 3-6.....	71
3-4	Results of the 50-foot tube length effect on the measured radon concentration using the testing setup of Figure 3-6.....	72

Table No. page

3-5 Soil samples identification system and corresponding sample configuration..... 106

3-6 Results of soil water weights and sample water contents for the original and processed soil samples collected at the three construction sites at three depths..... 107

3-7 A brief summary of the investigation approach, potential effect, and potential contribution to soil-gas radon testing result misrepresentation for testing (setup) configuration condition (A), temperature condition (B), soil compaction condition (C), and soil water content condition (D)..... 136

3-8 A brief summary of the recommendation for the degree of necessity to incorporate precaution or procedures developed in this research in designing, developing, and executing soil-gas radon testing to support the construction management decision for incorporating radon control system(s) installation prior to construction. Testing codes are: A = testing (setup) configuration condition, B = temperature condition, C = soil compaction condition, and D = soil water content condition..... 136

LIST OF FIGURES

Figure No.		page
1-1	Estimate of fatalities per year attributed to indoor radon exposure and its relative position with respect to fatality causes.....	11
1-2	Illustration of the first two states of radon in the soil representing radon availability.....	19
1-3	Illustration of the third and fourth states of radon in the soil representing radon migration.....	20
2-1	An illustration of the soil-gas radon testing system using photomultiplier-based instrumentation.....	44
2-2	A block diagram illustrating the experimental assembly used to test the effects of soil water content on soil-gas radon measurements.....	45
2-3	The linear correlation and operating range of the pressure measurement at the test chamber.....	49
2-4	The linear correlation and operating range of the relative humidity measurement at the test chamber.....	52
2-5	The linear correlation and the operating range of the temperature measurements at the test chamber.....	55

Figure No.		page
2-6	An illustration of the experimental setup to investigate tube-length effect on soil-gas radon testing.....	57
3-1	Average radon concentrations as a function of the soil-gas radon collection tube (or line) and the corresponding standard deviations.....	76
3-2	The maximum percentage of average radon concentrations that is attributed to statistical uncertainty of the measurement.....	78
3-3	Experimental and fitted relationships between the average radon concentration and the length of the radon collection tube of the soil-gas radon testing setup.....	80
3-4	The square root of the square of difference between the experimental average radon concentration and the predicted average radon concentration as a function of the collection tube length.....	82
3-5	Ratio of measured average radon concentration to zero-tube radon concentration per length of the collection tube.....	85
3-6	Predictions of the pressure differentials induced by temperature differences between two zones.....	90
3-7	A two-and-a-half-day temporal response of the temperature inside the testing chamber for the dried configuration sample of site S1 collected at a 3-foot depth.....	92

Figure No. page

3-8 A two-and-a-half-day temporal response of relative humidity measured inside the testing chamber during the testing of the dried configuration sample of site S1 collected at a 3-foot depth..... 93

3-9 A two-and-a-half-day temporal response of the differential pressure between the testing chamber and the surrounding air during the testing of the dried configuration sample of site S1 collected at a 3-foot depth..... 94

3-10 A two-and-a-half-day sample of the time-dependent temperature response in the testing chamber for the saturated soil sample collected from site 2 at a 4-foot depth..... 95

3-11 A two-and-a-half-day sample of the time-dependent relative humidity response in the testing chamber for the saturated soil sample collected from site 2 at a 4-foot depth..... 97

3-12 A two-and-a-half-day sample of the time-dependent differential pressure response across the testing chamber for the saturated soil sample collected from site 2 at a 4-foot depth..... 98

3-13 A two-and-a-half-day sample of the time-dependent temperature response in the testing chamber during the placement of the original soil sample collected at site 2 at a 2-foot depth..... 99

3-14 A two-and-a-half-day sample of the time-dependent relative humidity response in the testing chamber during the placement of the original soil sample collected at site 2 at a 2-foot depth..... 100

Figure No. page

3-15 A two-and-a-half-day sample of the time-dependent differential pressure response across the testing chamber during the placement of the original soil sample collected at site 2 at a 2-foot depth..... 101

3-16 Distribution of soil water content of the original soil samples collected at the three construction sites for depths of 2, 3, and 4 feet, respectively..... 111

3-17 Distribution of soil water content of the processed dried soil samples collected at the three construction sites for depths of 2, 3, and 4 feet, respectively..... 113

3-18 Distribution of soil water content of the processed saturated soil samples collected at the three construction sites for depths of 2, 3, and 4 feet, respectively..... 115

3-19 Illustration of the original, dried, and saturated soil samples water contents collected from 2 to 4 feet below grade from the three construction sites in Gainesville..... 116

3-20 The maximum range of soil moisture variation observed among original and processed samples collected from 2 to 4 feet below grade from the three construction sites in Gainesville..... 118

3-21 An illustration of the average radon concentrations measured at the testing chamber for the original soil samples collected from the three construction sites at depths of 2 to 4 feet..... 120

Figure No. page

3-22 An illustration of the average radon concentrations measured at the testing chamber for the dried soil samples collected from the three construction sites at depths of 2 to 4 feet..... 121

3-23 An illustration of the average radon concentrations measured at the testing chamber for the saturated soil samples collected from the three construction sites at depths of 2 to 4 feet..... 123

3-24 The maximum range of average radon concentration variations measured at the testing chamber for all soil samples collected from the three construction sites in Gainesville..... 124

3-25 The time-integrated response radon concentrations for original, dried, and saturated soil samples measured in the testing chamber..... 127

3-26 An illustration of the changes in the measured average radon concentration of original in-situ soil samples in response to the range of soil water moisture from dryness to saturation..... 130

Abstract of Dissertation Presented to the Graduate School of the University of Florida in Partial Fulfillment of the Requirements for the Degree of Doctor of Philosophy

EVALUATING THE EFFECTS OF SOIL AND ENVIRONMENTAL CONDITIONS FOR SOIL-GAS RADON TESTING PRIOR TO CONSTRUCTION

By

E. Salimi Tari

May 1999

Chairman: Dr. Fazil T. Najafi
Major Department: Civil Engineering

Exposure to elevated indoor concentrations of radon is among the greatest environmental hazards threatening the public health. The predominant source of indoor radon concentration is the soil beneath structures. The indoor radon problem, by definition, only exists once the structure is built. Although soil radon potential maps and other statistical approaches have been used to predict indoor radon problems, soil-gas radon testing provides the most direct and accurate method for assessing potential indoor radon problems.

Testing soil-gas radon concentration prior to construction is an emerging construction practice. Neither testing standards nor management practices have been developed

and recognized to ensure appropriate soil radon representation and testing administration. Accordingly, various setups may be used for the purpose of testing soil-gas radon concentrations. This research adapts the use of Pylon AB-5 with standard 300A scintillation cell that is coupled with the testing probe and the Pylon's suction pump through 5/16 I.D. Tubing. This testing apparatus is the most widely used setup in the industry for testing radon-soil gas concentrations. Using appropriate soil-gas testing procedures as a construction-management practice facilitates timely decisions on incorporating indoor radon prevention and control systems. This approach offers important advantages that include installation cost savings, design flexibility, reduced general liability, and improved public health.

Four conditions can contribute to invalidating the results of soil-gas testing: testing setup configuration, temperature, soil compaction, and soil water content. Experimental, theoretical, and managerial approaches have been utilized to investigate these conditions. The present research demonstrated the following conclusions.

(1) A soil-gas collection tube length can significantly affect reported radon concentration. Increasing the tube length results in reducing the soil-gas flow rate and consequently the measured radon concentration.

(2) Temperature differences have minimal effects on the reported radon concentration and do not cause significant

misrepresentation in test results.

(3) Soil compaction can significantly affect soil-gas radon testing, indicating that testing should be conducted before soil compaction at the construction site.

(4) Soil water content, encountered in normal environmental conditions, has only a minimal effect on the validity of soil-gas radon testing.

It should be noted that the components of the recommended construction-management approach in this research are based on the limitations of the above conditions and the experimental setup and testing procedures related to the testing apparatus referenced above. Accordingly, the findings and recommendations presented in this research should be viewed within the configurations limited by the scope of the referenced conditions and testing apparatus since they may not necessarily be valid for other configurations.

CHAPTER 1
INTRODUCTION AND LITERATURE SURVEY

Statement of the Problem

Radon and its progeny form the dominant source of the largest natural radiation dose that a person is naturally exposed to during his or her lifetime, mainly through inhalation into the lungs. Concern about indoor radon exposure in residential and commercial structures is relatively new and has evolved during the past fifteen years. While exposure to high concentrations of radon in uranium and other underground mines and its health effects were known and documented, it was only during the 1980s that residential structures with elevated radon concentrations were discovered.

In 1988, Congress passed the Indoor Radon Abatement Act that called for reduced public exposure to background levels of radon. Although reduction of radon concentrations in all residential and large buildings to background levels is not practically achievable, significant efforts have been devoted toward this goal.

Most efforts to control exposure to indoor radon have focused on mitigation in existing structures. Further, many procedures and systems developed for mitigating indoor radon

have focused on residential structures. Although research is underway to control radon exposure in large structures such as hospitals, office buildings, commercial buildings, and shopping centers, remediation of the indoor radon problem in large structures is much less developed than for residential structures.

Due to the cost associated with controlling indoor radon problems, significant savings can be realized if appropriate procedures and systems are implemented during the construction phase and before the building is completed. Therefore, development of radon-resistant construction standards for both residential and commercial buildings has been heavily pursued.

Nevertheless, one important problem exists. The indoor radon problem, as the name indicates, only exists after a structure is built and the indoor space is established. The space is defined upon issuance of a certificate of occupancy. Testing for radon in the soil can only indicate a potential problem.

The significant cost savings from installing radon-control systems during construction indicates a need to develop procedures and approaches to test for soil-gas radon concentration. Upon discerning the concentration, a decision can be made to incorporate passive and/or active radon-control systems. Despite this need, apart from testing for indoor radon concentrations, no standards have been developed for testing radon concentrations in soil.

Furthermore, testing of soil gas prior to construction is subject to several factors that might affect the test results. This is the primary factor in deciding to incorporate radon-control features in structures. This research addresses the factors that might affect testing of soil-gas radon concentration prior to construction, as well as the testing procedures, for the purpose of developing a construction-management approach to soil-gas radon testing prior to construction.

Objectives of the Research

The first objective of this research is to evaluate the effects of soil and environmental conditions including temperature, soil moisture, pressure, and testing device characteristics used for and associated with the measurement of soil-gas radon concentration prior to construction.

The second objective is to develop a construction-management approach that can be used by construction and design contractors, consultants, and any other interested party to coordinate testing of soil-gas radon concentration prior to construction.

The third objective is to determine testing procedures for soil-gas radon concentrations that can be used prior to construction by incorporating currently available radon-

measurement technology and to determine appropriate testing conditions, including soil and environmental conditions.

Properties of Radon

Radon (Rn) is a gas formed from the radioactive decay of radium (Ra). Radium is part of the naturally occurring radioactive decay series of uranium (U-238 and U-235) and thorium (Th-232). Radioactive disintegration of these elements produces three isotopes of radon: ^{222}Rn, ^{220}Rn, and ^{219}Rn; with half-lives of 3.825 days, 55.6 seconds, and 3.92 seconds, respectively.

Radon is a noble or inert odorless and colorless gas that is approximately ten times heavier than air. It is the heaviest element in the inert gases column in the periodic table. In this position, radon has the highest critical pressure, critical temperature, boiling point, and melting point among inert gases.

Because radon is an inert gas, its chemical properties are extremely limited and its chemical reactions with soil, concrete, carpet, and other materials available in the indoor environment do not exist in environmental conditions. Table 1-1 gives some selected physical properties of radon.

Radon isotopes are usually in secular equilibrium with their parents in the environment. In radiological terms, ^{222}Rn (from the decay of ^{226}Ra) is the most important among radon

radonisotopes. ^{222}Rn has the longest half-life and its parent (uranium series) is the most abundant among radon isotopes' parents in geological materials.

^{222}Rn decays to ^{218}Po by releasing an alpha particle of 5.49 million electron-volt (MeV) that can be described by the following equation:

$$^{222}Rn \text{ ---------} \rightarrow {}^{218}Po + {}^{4}He + 5.49 \quad (MeV)$$

Table 1-2 gives the radionuclide, half-life, alpha and beta particles' decay energies for part of the U-238 decay chain starting with Ra-226. Polonium-218 in the above equation disintegrates into Lead-214, releasing an alpha particle of 6.00 MeV as seen in the table. Polonium-218, Lead-214, Bismuth-214, and Polonium-214 are called the immediate daughters or progeny of the isotope Rn-222.

The immediate progeny carry the significant part of radiation that is delivered to human lungs upon inhalation of radon. They are chemically very active elements, and all have relatively short half-lives of less than 30 minutes. This characteristic makes these radionuclides radiological toxins, as they will disintegrate within the time frame needed to complete one breathing cycle by the normal lung-clearance mechanism. Thus, they can decay to ^{210}Pb, which has a half-life of 22.3 years.

Health Hazards of Indoor Radon Exposure

Potential health problems from exposure to indoor radon result from dose accumulation due to inhaling radon and its immediate progeny. Deposits of radon progeny inside the lungs could build up to levels that directly contribute to the development of lung cancer over a period of time.

Radon has been classified as a Group A carcinogen in humans, with sufficient evidence that it causes cancer, based on data from epidemiologic studies and underground miners. Exposure to radon has been declared a major public health concern by many national and international organizations. These include, but are not limited to: the U.S. Environmental Protection Agency (USEPA 1992); the National Academy of Science (NAS), through the Biological Effects of Ionizing Radiation (BEIR IV) Committee (NAS 1988); the World Health Organization (WHO), through the International Agency for Research and Cancer (IARC 1988); the National Council on Radiation Protection and Measurement (NCRP 1984); the International Commission on Radiological Protection (ICRP 1987); the Centers for Disease Control and Prevention (CDC); the American Medical Association (AMA); the American Lung Association (ALA); and the American Public Health Association (APHA). Since radon and its progeny are mainly alpha emitters, the accumulated dose received by the lungs is generated from alpha particles' decay.

Table 1-1: Selected physical properties of radon

Property[a]	Value
Boiling point (°C)	-61.8
Critical temperature (°C)	104.0
Critical pressure (atmosphere)	62.0
Density (at normal pressure and temperature) (kg/m^3)	9.96
Melting point (°C)	-71.0
Vapor pressure (at 99.0°C) (kPa)	13.0
Vapor pressure (at 61.8°C) (kPa)	100.0
Solubility coefficient in water (atmospheric pressure, 100°C)	0.106
Solubility coefficient in water (atmospheric pressure, 0 °C)	0.507

[a] modified from (UNSC 1982)

Table 1-2: Major characteristics of ^{222}Rn and its decay products (part of ^{238}U decay chain)

Radionuclide	Half-Life	Alpha (MeV)	Beta (MeV)
Ra-226	1600y	4.06, 4.78	
Rn-222	3.825d	5.49	
Po-218	3.11m	6.00	
Bi-214	19.9m		3.27, 1.54, 1.5
Po-214	164μs	7.69	
Pb-210	22.3y		0.02, 0.06
Bi-210	5.01d		1.16
Po-210	138d	5.03	
Pb-206	stable		

Alpha radiation has the highest quality factor for depositing its energy into living tissues, compared to other radiations. Thus, the radiological significance of radon exposure arises from two factors:
(1) radon is a chemically inactive gas but has a half-life that is long enough to easily reach and decay in the lung during inhalation; and (2) once radon has decayed in the lung, its progeny are chemically very active and have short half-lives that allow them to attach easily to the lung tissue and deposit most of their decay energy into tissues.

More evidence can be found in recent studies supporting the belief that ^{222}Rn is the major contributor to the radon health concern (NAS 1988). For this reason, radon in this work shall refer to ^{222}Rn.

The major radiological risk of inhaled radon and its decay products is the development of lung cancer. Lung cancer of the respiratory tract has emerged as the most common form of lethal cancer. It is estimated that lung cancer accounts for approximately one-fifth of all cancer deaths yearly in the United States (James 1984).

The EPA has estimated that radon is responsible for about 14,000 deaths per year (with a possible range of 7,000 to 30,000) and that it is the second leading cause of lung cancer in the United States. Estimates of the possible number of deaths in a sample of 100 persons versus exposure to different levels of radon concentration is shown in Table 1-3. The

expectations are based on the independent effects of radon compared to other risk factors, such as smoking. Smoking will significantly enhance the radon risk factor. The sample is adult persons; children may be at higher risk (USEPA 1992).

The position of radon as a cause of death with respect to other causes as reported by the 1990 National Safety Council reports is shown in Figure 1-1. Table 1-4 shows the risk of radon exposure for smoking, while Table 1-5 shows the risk for nonsmoking populations. The equivalent risks corresponding to fatality rates shown in Figure 1-1 are also given in Tables 1-4 and 1-5.

Finally, it is important to note that induction of cancer in biological systems is believed to be a stochastic process. Thus, exposure to radon does not by itself create cancer but rather increases the probability of cancer. This probability increases with the increase in the radiation dose and the exposure time.

Although concern is mainly for the isotope ^{222}Rn, small concentrations of ^{220}Rn may be available in the indoor area, especially in areas where soil has a noticeable concentration of thoron. In it, the decay of the short-lived daughter ^{220}Rn also contributes to the total dose delivered by inhaling radon gas.

Table 1-3: The risk of exposure to annual radon levels

Annual[a] radon level (pCi/l)	Sample of 100 people (possible deaths %)	Radon risk of lung cancer compares to . . .
100	(27-63)%	having 2,000 chest x-rays each year.
40	(12-38)%	smoking 2 packs of cigarettes each day.
20	(6-21)%	smoking 1 pack of cigarettes each day.
10	(3-12)%	having 500 chest x-rays each year.
4	(1.3-5)%	smoking half a pack of cigarettes each year.
2	(0.7-3)%	having 100 chest x-rays each year.

[a] modified from (EPA 1986)

Availability of Radon in the Soil Gas

The focal concern in this research is the availability of radon in a gaseous phase in the porous soil medium in which soil-gas radon is to be tested. Geologically, uranium is the umate source of radon in the soil. The following is the process by which radon is generated, starting from uranium.

It has been noted above that radon is generated from radium, which is a decay product in the uranium series. All rocks contain some uranium, with quantities estimated as 1-3 parts per million (ppm). The rocks break down due to environmental, mechanical, and chemical weathering factors to form soils at the earth's surface.

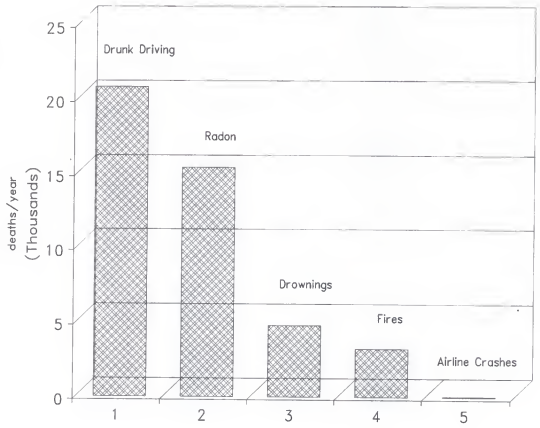

Figure 1-1: Estimate of fatalities per year attributed to indoor radon exposure and its relative position with respect to fatality causes

Table 1-4: Possible number of lung cancers and comparison of the risk of radon exposure for smokers

on level (pCi/l)	Possible number of lung cancers per 1000 people (lifetime exposure)	Radon exposure risk of cancer compares to . . .
20	135	100 times the risk of drowning.
10	71	100 times the risk of dying in a home fire.
8	57	80 times the risk of dying in a home fire.
4	29	100 times the risk of dying in an airplane crash.
2	15	2 times the risk of dying in a car crash.
1.3	9	(average indoor radon level)
0.4	3	(average outdoor radon level)

Since the uranium content of the generated soils has to be about the same as in the forming rocks, uranium concentrations in the soil average between 1-3 ppm.

Construction materials used in structures, for foundations and walls and so forth, that are prepared from processed geological materials contain some percentage of radium that is derived from predecessor radioisotopes in the earth materials. Earth materials such as light-colored volcanic rocks, granite, dark shales, phosphate-bearing sedimentary rocks, and metamorphic rocks contain

Table 1-5: Possible number of lung cancers and comparison of the risk of radon exposure for nonsmokers

Radon level (pCi/l)	Possible number of lung cancers per 1,000 people (lifetime exposure)	Radon exposure risk of cancer compares to ...
20	8	the risk of being killed in a violent crime.
10	4	half the risk of being killed in a violent crime.
8	3	10 times the risk of dying in an airplane crash.
4	2	the risk of drowning.
2	1	the risk of dying in a home fire.
1.3	<1	(average indoor radon level).
0.4	<1	(average outdoor radon level).

higher-than-average uranium percentages. These rocks and their soils contain as much as 100 ppm of uranium (USDOI 1992).

Radon in soils can be classified into two fundamental categories relative to its conditions in the soil. These categories are the availability of radon gas in the soil and the migration of the gas in the soil system (Al-Ahmady 1995). Each category consists of two states of radon in terms of its potential in the indoor environment. The availability of

radon in soil consists of the radon generation state and the radon in soil pores state.

The other category of radon migration in the soil system consists of migration in the soil state and entry into the structure state. The conditions in which radon may be classified in soil are complicated and affected by many parameters.

Radon can move from one state to another by transition processes that operate between two states. These processes are affected by many parameters, most of which are interrelated. Figures 1-2 and 1-3 illustrate the radon state in the soil, the transition processes, and the factors affecting these transitions (Al-Ahmady 1995).

Since radon is generated from the radioactive decay of ^{226}Ra, which is a solid, the initial location and thus the generation site for radon atoms must be within the soil grains. For the radon to be in the soil gas, the gas occupying the pore space of the soil, radon atoms generated in the grain must move toward and become trapped in the pore space to be included in the soil gas.

The transition process controlling this transfer is called radon emanation, and it is characterized by the radon emanation coefficient. This is defined as the percentage (or fraction) of radon that is available in the pore space of the soil to that originally generated in the soil grains. For most soils, only 10-50% of the radon produced in the first

state actually emanates from the mineral grain and enters the pore volume of the soil (USDOI 1992).

Among the factors that could influence radon emanation, soil moisture content may have a significant impact (Strong and Levins 1982). Calculations show that the radon atom recoils with an average kinetic energy of 86 keV (Bossus 1984). Thus, the relative position of formation and the direction of the recoil determine if the formed radon atom will terminate its path in the soil pore space.

The location characteristic where the path termination occurs is called the host material. This could be the solid grain of the formation, another solid grain, or materials confined in the soil pore, primarily water and air (Al-Ahmady 1995).

The range of the newly formed radon atom is the distance the atom travels between the formation point in the mineral grain and the termination point in the host material. This range depends on the density and composition of the host materials, the relative location of formation in the mineral grain, and the direction of the recoiled radon atom. The range of radon is 63 μm in air and 0.1 μm in water (Tanner 1980). Therefore, its range in water is approximately 600 times less than the range in air.

If the pore soil space is theoretically assumed to be filled with dry air (no water vapor), its availability is expected to significantly influence whether the recoil radon

atom terminates its range in the soil pore space. Fluid-filled soil pores contain most of the soil moisture. When the content of water in the pore space increases, the direct emanation coefficient component increases because a greater fraction of the recoil radon atoms are trapped in the pore.

The transition processes controlling the radon-emanating fraction in the soil are affected by soil moisture, soil temperature, soil grain-size distribution, and the intragranular location of radium atoms as seen in Figure 1-2 (Al-Ahmady 1995). The interagranular location of radium atoms and the soil grain-size distribution are not controlled during construction.

For the purpose of this research, the above two soil characteristics are considered to be there and are not related to the testing process itself. Soil moisture and soil temperature can be changed from day to day depending on environmental parameters; thus their effects on the soil-gas radon testing must be considered.

Soil moisture content can be analyzed in three components: capillary, gravitational, and gyroscopic. The capillary component represents films of water around the solid soil grains that develop from the capillary properties of liquids with narrow channeling and surfaces. The gravitational component represents the bulk of the water in the soil system that is affected by gravitational forces. The gyroscopic component of soil moisture is derived from the

electrostatic attraction between electrical charges on water and the solid soil grain; it consists of only a very small amount of the water in the soil and often is embedded within the solid soil grain.

Most of the soil moisture effect is developed by the capillary component of soil moisture water. This component is responsible for generating water films around solid grains that act as a trap for recoiled radon atoms (Al-Ahmady 1995).

If water in soil exists in excess of the capillary water component, only a minimal effect on the radon emanation occurs, since most of the atoms are being stopped by the capillary water films. The gyroscopic component also has a minimal effect on emanation, since it represents a very small percentage of soil moisture. Therefore, the capillary water component among soil moisture components may carry the potential to alter soil-gas testing results. This component will be experimentally examined for that purpose.

Al-Ahmady (1995) describes three components in explaining the emanation of the radon atom from the solid soil grain into its surroundings. These are the direct recoil, indirect recoil, and diffusion components. The diffusion component refers to the recoil radon atoms that terminate their paths in the same solid grain where they formed and migrate into the pore space through molecular diffusion. The indirect component refers to the percentage of generated radon atoms that traverse the soil pore space, penetrate another grain,

and end their paths in that grain. The direct component refers to the percentage of the recoiled radon atoms that terminate their paths in the soil pore spaces.

Once the radon enters the soil pore space, it becomes migratory. Soil permeability and diffusion length are the two factors affecting the transition of radon in soil pore state to the next state of migration in the soil. Soil permeability is the most important soil characteristic that affects indoor radon concentrations. This soil parameter measures how readily the soil gas, or generally a fluid, may flow through the soil. It is traditionally represented in units of area. The permeability of soil changes significantly over the range of 10^{-7} m^2 for highly permeable soils, such as clean gravel, to values on the order of 10^{-16} m^2 for very low permeability soils such as homogenous clays.

Since soil permeability regulates fluid flow in porous soil media, it relates the flow with the pressure gradient. Customarily, intrinsic soil-gas velocity is used as an indicator of the quantity of soil gas with regard to indoor radon concentration.

The broad range of soil permeabilities makes this parameter important to the transport of radon-rich soil gas from the substructure area into the indoors and consequently to the indoor radon concentration.

Furthermore, because soil permeability is highly inhomogeneous, this parameter is difficult to model.

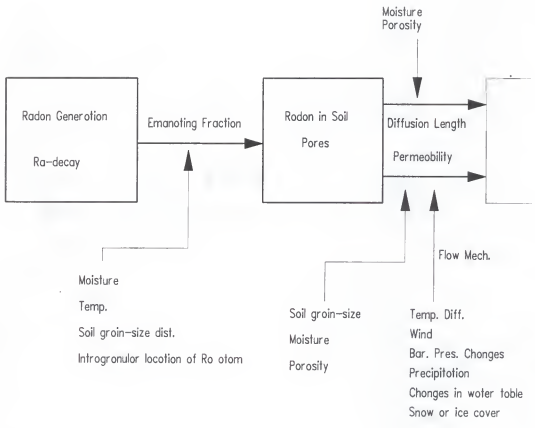

Figure 1-2: Illustration of the first two states of radon in the soil representing radon availability

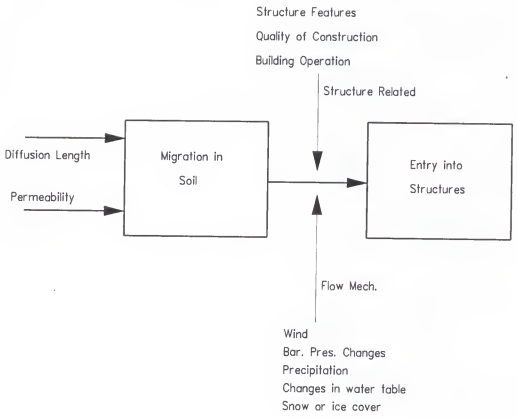

Figure 1-3: Illustration of the third and fourth states of radon in the soil representing radon migration

At high permeability values, convective soil-gas transport becomes the dominant transport mechanism permitting increased radon entry and, generally, increased indoor radon concentrations. At low permeability values, convective flow is minimal and molecular diffusion transport of soil gas is dominant.

The second parameter regulating soil-gas transport in porous soil media is the diffusion length. Radon diffusion length in soil depends on both soil water content and soil porosity. Diffusion length is a characteristic parameter of radon diffusivity in the soil that is driven by concentration gradients and facilitated by molecular diffusion. It relates the radon diffusive flux to the radon concentration gradient. This relationship is governed by Fick's law. When the latter relation is utilized, the mathematical representation of radon diffusion length is usually replaced by the radon diffusion coefficient (Al-Ahmady 1995).

In a porous medium, there are four formats of radon diffusion coefficients that can be used depending on the type of physical soil quantities utilized. A descriptive quantity of bulk versus pore volumes to determine concentration and bulk versus pore volumes to determine density results in a bulk and effective, or intrinsic, diffusion coefficient.

The effective diffusion coefficient relates the gradient of the interstitial radon concentration to the radon flux density calculated across the pore soil area (Al-Ahmady 1995).

The radon bulk diffusion coefficient relates radon flux density to the gradient of interstitial radon concentration calculated across a geometric or superficial area. When soil moisture increases, a high percentage of pore space is blocked, reducing the radon diffusion in the soil. Researchers have concluded that increasing soil moisture reduces the radon diffusion coefficient, while increasing the soil porosity increases the radon diffusion coefficient (Rogers et al. 1984).

Radon Transport in Soils

A system approach has been utilized for conducting this research. With the focus on the construction-management approach prior to construction and the associated testing procedures, the details of transport of radon in the soil system is a secondary aspect of this work.

Details of the transport of radon in soils would be of primary importance for researching the fate and movement of radon for different purposes. However, mathematical consideration for radon transport in soils is discussed in this chapter as an integral background for future research. The terminology and primary coverage of the subject is adapted from Al-Ahmady (1995).

The transport of radon, as other chemicals, in soil results from movement of the source before generation and from

diffusion and convective flows after generation. Since distribution of a radon source is considered uniform, consideration is given to the transport mechanisms once radon is generated, mainly those related to transporting recoiled radon atoms from the mineral grain into the pore space. Those mechanisms also result in transporting gaseous radon in the soil pore space collectively.

The random molecular motion of a substance due to its concentration gradient is best represented by Fick's law as a diffusional flux density. The convective components of radon transport, which primarily results from pressure differentials, can be represented by Darcy's law. Convective flow of radon is more significant to the transport of the gas from the soil system into the indoor space. The latter is not a consideration in this research. However, differential pressure may exist between the measurement system and the location where soil gas is collected.

The effect of possible changes in the differential pressure between the collection system and in-situ location is considered through experimental verification outlined in the methodology section of this work.

If a coordinate system is chosen at a certain in-situ location in the soil and remains stationary, the flux density of a substance (identified as gas 1) in a mixture of two gases (1 and 2) can be given as

$$N_1 = f_1 (N_1+N_2) - C D_b \nabla f_1 \qquad (1\text{-}1)$$

where

N_1 is the molar flux of gas 1 (moles/m²s),

N_2 is the molar flux of gas 2 (moles/m²s),

f_1 is the molar fraction of gas 1 in the mixture,

C is the molar concentration of the gas (moles/m³),

D_b is the binary diffusion coefficient (m²/s), and

∇ is the three-dimensional gradient operator.

In the above equation, the second term represents the molecular diffusion component relative to the mean convective velocity, and the first term represents the convective transport component.

In the molecular diffusion process, the dominant driving force of gas molecular movement between two areas is the concentration difference of the gas between these two areas. Therefore, the second term in Equation 1-1 is constructed based on Fick's first law, governing the relation between the concentration gradient and the diffusional flux density.

If the gas labeled as 2 is the soil gas and 1 is radon, then N_1 represents the molar flux density of radon. Radon is considered here within the assumption of a binary mixture in the soil gas. This neglects the effect of the transport of radon that may result from the diffusion of one or several other species in the soil gas. However, the effects of this

multicomponent diffusion in radon transport are minimal for soil-structure configurations dominated by the convective transport of soil gas (Nazaroff et al. 1988).

Since the objective of this treatment is to generally address radon transport in the soil system and not the details of molecular diffusion phenomena, an effective diffusion coefficient (D_e) is systematically assumed. The latter can be used to replace the binary diffusion coefficient (D_b).

Under normal conditions, the mole fraction of radon isotopes in the soil gas is nearly equivalent to the mole fraction of ^{222}Rn (7.6×10^{-16} at 20 °C), which is small compared to the soil gas (Nazaroff et al. 1988). Therefore, if the molecular diffusion of radon in the soil as a source of convection in the mixture is neglected, then N_1 can be neglected compared to the soil-gas flux density N_2. This assumption results in reducing Equation 1-1 to

$$N_1 = f_1 N_2 - C D_e \nabla f_1 \qquad (1\text{-}2)$$

If the molar concentration of soil gas remains constant in time and space, then

$$N_1 = f_1 N_2 - D_e \nabla C f_1 \qquad (1\text{-}3)$$

or

$$N_{Rn} = f_{Rn} N - D_e \nabla (C f_{Rn}) \qquad (1\text{-}4)$$

where N is the molar flux density of the soil gas (air) in the soil pore space.

It is customary to treat radon quantities in terms of activity, since this is ultimately the major concern with regard to the radon health hazard. Terms in Equation 1-4 need to be multiplied by Avogadro's number (A_v) and the decay constant of radon (λ_{Rn}) to convert the molar flux density and molar concentration density into activity flux density and activity concentration density, respectively.

Then

$$A_v \lambda_{Rn} N_{Rn} = [f_{Rn} N - D_e \nabla f_{Rn} C] A_v \lambda_{Rn} \quad (1\text{-}5)$$

Dividing Equation 1-5 by the molar fraction of Rn in the soil gas yields

$$\mathbf{A}_f(Rn) = A_m(Rn) \frac{N}{C} - D_e \nabla A_m(Rn) \quad (1\text{-}6)$$

where

$A_f(Rn)$ is the radon activity flux density (Bq/m^2s), and

$A_m(Rn)$ is the radon activity concentration density (Bq/m^3).

The value of N/C in the first term of Equation 1-6 has units of velocity (m/s), and it is equivalent to the net soil gas velocity, so it can be replace by the symbol V,

$$\mathbf{A}_f(Rn) = A_m(Rn) \mathbf{V} - D_e \nabla A_m(Rn) \quad (1\text{-}7)$$

Equation 1-7 contains two transport terms. The first term ($A_m(Rn)V$) is the convective flux, and the second term ($-D_e \nabla A_m(Rn)$) is the diffusive flux.

Further assumptions must be made in order to apply Equation 1-7 in a complex soil system. In fact, to account for the effect of the soil fill materials and near-structure conditions, an effective diffusion coefficient has already been assumed. Further, these conditions increase the radon mean free path. This increase is not helpful for the soil porosity considerations which were assumed in developing the above equations, since radon atoms are assumed to be interacting with soil gas molecules (gaseous state). However, support for this assumption can be derived from the fact that soil pores are relatively larger than the applicable average radon mean free path, which assures that the assumption is reasonable.

It is typically assumed that pore dimensions are comparable to the size of mineral grains. Since the required size should be comparable to the soil gas (compared to the air of 0.065 micrometer at 25°C), the diffusion term can be applied to the soils of grain size on the order of approximately 0.065 micrometer or larger, which in fact covers all soils larger than clays. Testing of soil-gas radon concentration for the purpose of developing a potential indicator cannot be facilitated in soils that have significant amounts of clay.

Since radon is an almost chemically inert gas and the average environmental temperatures are much higher than its

condensing temperature, the diffusion process in the soil is dominated by gaseous radon diffusion.

Radon transport by diffusion in liquid and solid phases can be neglected for most practical applications (Al-Ahmady 1995). Support for this assumption can be found in experimental results, which show insufficient evidence to consider these effects important (Tanner 1980).

The dominant driving force for the convective radon transport component is the pressure differentials. Darcy's law describes the volume of interstitial fluid flowing per unit of time per unit of geometrical area as a result of an applied pressure differential, or the velocity vector. If the geometrical area in the soil, where the flow is defined, is small compared to the overall dimension of the soil and large compared to the individual pores, then the net superficial velocity vector can be written as

$$\boldsymbol{V} = -\frac{[K]}{\mu}\nabla P \qquad (1\text{-}8)$$

where

[K] is the three-dimensional permeability matrix,

μ is the viscosity of the fluid, and

P is the pressure.

If the soil permeability is constant and isotropic, the three-dimensional permeability matrix becomes the permeability coefficient K. Further adjustments can be made by dividing V by the soil porosity e, which is a dimensionless fraction

representing the ratio of the air and water porosity to the bulk volume. Substituting V in the convective component of Equation 1-7, the superficial air velocity through the soil expressed in term of Darcy's law per unit pore area yields

$$\mathbf{A_f}(Rn) = A_m(Rn)\frac{\boldsymbol{V}}{e} - D_e \nabla A_m(Rn) \qquad (1\text{-}9)$$

Substituting Equation 1-8,

$$\mathbf{A_f}(Rn) = -A_m(Rn)\frac{K}{\mu e} \nabla P - D_e \nabla Am(Rn) \qquad (1\text{-}10)$$

divided into two terms,

$$A_f^c(Rn) = -A_m(Rn) \frac{K}{\mu e} \nabla P \qquad (1\text{-}11)$$

$$A_f^d(Rn) = -D_e \nabla A_m(Rn) \qquad (1\text{-}12)$$

then

$$\mathbf{A_f}(Rn) = A_f^c(Rn) + A_f^d(Rn) \qquad (1\text{-}13)$$

\

where

A_f^c(Rn) is the radon activity flux density per unit pore area due to convection, and

A_f^d(Rn) is the radon flux density due to molecular diffusion.

The nature of radon flux density removal mechanisms by both molecular diffusion and convection can be characterized by radon transport from a differential volume in a direction perpendicular to a volume surface area. The total radon diffusion from the differential volume can be calculated by integrating both fluxes over the total differential surface

area. This integration is equivalent to integrating the divergence of these fluxes over the total differential volume, according to the divergence theorem,

$$\int_s A_f^d(Rn)\ ds = \int_v \nabla A_f^d(Rn)\ dv$$
$$\int_s A_f^c(Rn)\ ds = \int_v \nabla A_f^c(Rn)\ dv \qquad (1\text{-}14)$$

The limitation on $A_f^c(Rn)$ is determined by the dependence of Darcy's law on the Reynolds number. Usually, Darcy's law starts to give incorrect results for high values of the Reynolds number. Scheidegger has provided experimental evidence showing that applications of Darcy's law for Reynolds numbers smaller than 76 are acceptable (Scheidegger 1960). The typical pressure gradients in the soil due to air flow into structures results in Reynolds numbers much smaller than 76. Therefore, Darcy's law is approximately correct for radon transport applications.

A general transport equation that describes radon transport in the soil can be developed by considering the rate of change in the quantities of production, convective flow, molecular diffusion and decay. Under the limitations that arise from the application of Fick's law for molecular diffusion and Darcy's law for convective transport, the time rate of change in the radon activity concentration in the pore, for soils of low moisture content, can be written as

$$\int_v \frac{\partial A_m(Rn)}{\partial t}\, dv = -\int_s A_f^c(Rn)\, ds - \int_s A_f^d(Rn)\, ds - \int_v \lambda_{Rn} Am(Rn)\, dv + \int_v S\, dv \qquad (1\text{-}15)$$

where

S is the volumetric radon source term in (Bq/m^3), and

λ_{Rn} is the radon decay constant ($2.1x10^{-6}$ disintegration/s for ^{222}Rn).

The radon source term is the production of radon which occurs in the interstitial space of the soil and has free transport through the pore spaces. The production rate can be written as

$$S = \left(\frac{1-\epsilon}{\epsilon}\right) A(Ra)\, \lambda_{Rn}\, f_e\, \rho_s \qquad (1\text{-}16)$$

where

A(Ra) is the mass activity of radium concentration in the soil in (Bq/kg),

f_e is the emanation factor, the fraction of the radon that is generated in the soil and enters the pore volume,

ρ_s is the soil grain density in (kg/m^3), and

ϵ is the soil porosity. Substituting equations 1-11, 1-12, and 1-16 into 1-15 yields

$$\int_v \frac{\partial A_m(Rn)}{\partial t}\, dv = \int_s A_m(Rn)\ \frac{K}{\mu\varepsilon}\ \nabla P\, ds + \int_s D_e\, \nabla A_m(Rn)\, ds - \int_v \lambda_{Rn}\, A_m(Rn)\, dv + \int_v (\frac{1-\varepsilon}{\varepsilon})\ A(Ra)\ \lambda_{Rn}\ f_e\ \rho_s\, dv \qquad (1\text{-}17)$$

Using Equation 1-14 for the total diffusion and convective integral terms results in

$$\int_v \frac{\partial A_m(Rn)}{\partial t}\, dv = \int_v \nabla A_m(Rn)\ \frac{K}{\mu\varepsilon}\ \nabla P\, dv + \int_v D_e\, \nabla^2 A_m(Rn)\, dv - \int_v \lambda_{Rn} A_m(Rn)\, dv + \int_v \frac{1-\varepsilon}{\varepsilon}\ A(Rn)\ \lambda_{Rn}\ f_e\ \rho_s\, dv \qquad (1\text{-}18)$$

or

$$\frac{\partial A_m(Rn)}{\partial t} = A_m(Rn)\ \frac{K}{\mu\varepsilon}\ \nabla^2 P + D_e\, \nabla^2\ A_m(Rn) - \lambda_{Rn}\ A_m(Rn) + (\frac{1-\varepsilon}{\varepsilon})\ A(Ra)\ \lambda_{Rn}\ f_e\ \rho_s \qquad (1\text{-}19)$$

Equation 1-19 is the differential form of the general transport equation for radon transport in soil.

The equation can cover a certain area by integrating all terms over that specific area. Notice that the equation has time and space partial derivatives, which complicate the analytical solution. Equation 1-19 can be solved analytically for only simple geometries, requiring many assumptions. For realistic conditions, numerical methods must be used.

Several assumptions can be made to simplify Equation 1-19; for example, the steady state solution is based on eliminating the time rate of change of the activity of radon concentration, that is, the left-hand side of Equation 1-19 becoming zero.

To examine the effect of each term in Equation 1-19 for particular applications, the molecular diffusion term can be simplified. An example would consider one-dimensional (z-axis) radon diffusion in soil without the effects of the structure, that is, uncovered soil and low moisture content. If the radon activity concentration is assumed to be zero at the surface of the soil and the radon source is located at an infinite depth in the soil, then the radon activity concentration at depth z can be given by

$$A_m^z(Rn) = A_m^*(Rn)\ (1-e^{-\frac{z}{l_{Rn}}}) \qquad (1\text{-}20)$$

where

$A_m^z(Rn)$ is the radon activity concentration at z,

$A_m^*(Rn)$ is the initial activity concentration, and

l_{Rn} is the radon diffusion length.

The radon diffusion length and the initial concentration can be given as

$$l_{Rn} = \sqrt{\frac{D_e}{\lambda_{Rn}}} \qquad (1\text{-}21)$$

and

$$A_m^{\circ}(Rn) = \frac{S}{\lambda_{Rn}} \tag{1-22}$$

Using Equation 1-16 results in

$$A_m^{\circ}(Rn) = \left(\frac{1-\epsilon}{\epsilon}\right) f_e \rho_s A(Ra) \tag{1-23}$$

Substituting Equations 1-20 and 1-23 into 1-12 yields

$$A_f^d(Rn) = -D_e \frac{1-\epsilon}{\epsilon} f_e \rho_s A(Ra) \nabla\left(1-e^{-\frac{z}{l_{Rn}}}\right) \tag{1-24}$$

and substituting Equation 1-21 into 1-24, for the one-dimensional case, yields

$$A_f^d(Rn) = \frac{1-\epsilon}{\epsilon} f_e \rho_s A(Ra) \sqrt{D_e \lambda_{Rn}} \tag{1-25}$$

The diffusive radon activity flux density per unit of geometric area is given by multiplying Equation 1-25 by the soil porosity ϵ,

$$A_f^d(Rn) = (1-\epsilon) \rho_s f_e A(Ra) \sqrt{D_e \lambda_{Rn}} \tag{1-26}$$

The radon activity flux density is related to the radon activity concentration by Fick's law through the effective diffusion coefficient, as shown in Equation 1-12. The differential radon activity flux density from the molecular diffusion in Equation 1-26 is in fact the application of Equation 1-12 on a solution, for $A_m(Rn)$, in the following partial differential equation. Describing the radon transport in soil by diffusion only,

$$\frac{\partial A_m(Rn)}{\partial t} = S - \lambda_{Rn} A_m(Rn) + D_e \nabla^2 A_m(Rn) \qquad (1\text{-}27)$$

Substituting Equation 1-16 into 1-27 yields

$$\frac{\partial A_m(Rn)}{\partial t} = \left(\frac{1-\epsilon}{\epsilon}\right) A(Ra)\, \lambda_{Rn}\, f_e\, \rho_s - \lambda_{Rn} A_m(Rn) + D_e \nabla^2 A_m(Rn) \qquad (1\text{-}28)$$

Notice that Equation 1-28 is identical to Equation 1-19 except for the convective transport term being absent.

Applying typical values for ^{222}Rn in Equation 1-26 results in radon activity flux densities on the order of $(10\text{-}20) \times 10^{-3}$ (Bq/m^2s). Wilkening et al. estimated values of the mean ^{222}Rn activity flux density of approximately 0.015 Bq/m^2s, from data collected on widely spread regions (Wilkening et al. 1972). Nazaroff et al. provided the radon activity flux, using typical values such as $\rho_s = 2.65 \times 10^3$ kg/m^3, $f=0.2$, $\epsilon=0.5$, $D_e = 2 \times 10^{-6}$ m^2/s and radium mass activity of 30 Bq/kg, as 0.016 Bq/m^2s (Nazaroff et al. 1988).

CHAPTER 2
METHODOLOGY AND EXPERIMENTAL DESIGN

Scope of the Methodology

The purpose of this section is to outline the scope of research to permit the development of a construction-management approach and the associated testing procedures. These procedures are directed toward helping the decision process of electing to install radon control systems based on soil-gas radon testing prior to construction.

When considering the components of the testing process and validation of test results to facilitate the management decision, there are four areas where research is needed. Those areas are mainly related to the physical conditions that might affect the testing results. The timing and scheduling of the tests also are factors that need to be considered, but they relate more to management than to the technical aspects of the implementation process.

Physical conditions that might affect the testing of soil-gas radon concentration prior to construction are:

(1) the condition of soil moisture;

(2) the condition of temperature difference between the testing system and the soil;

(3) the condition of the testing configuration; and

(4) the condition of soil compaction.

As to the first condition, related to soil moisture, some theoretical results have established that soil moisture can significantly alter the emanation of radon. Existence of moisture in the pore space of the soil affects the range of the radon atom's transport and thus the final destination of the recoiled atom. This determines whether the recoiled atom terminates its path in the pore space and thus becomes capable of migrating. Only radon in a gaseous phase can become mixed and carried with soil gas.

The subject of this research is not the details of the process of emanation or radon transport as related to soil moisture, but rather the investigation of the effect that soil moisture would have on soil-gas radon during the testing based on a system approach. In other words, the research task on soil moisture is designed to answer the question of whether soil moisture would invalidate soil-gas radon moisture prior to construction as a representative indicator in the management decision. If invalidation is established, then the management approach must accommodate this effect and require testing of specific conditions to avoid the potential for misrepresentation.

It should be noted that the approach does not consider creating the perfect conditions but rather is to develop the procedure that best represents the soil conditions. Soil

water moisture is not an issue of control; it is a characteristic of the site that can vary periodically or on a relatively immediate basis, such as after a heavy rain.

The focus is whether testing of soil-gas radon prior to construction, when used as an indicator for a construction-management decision, should be avoided or rescheduled due to abnormal soil moisture conditions. Alteration to natural or normal soil moisture conditions as related to the soil-gas radon testing could occur, for example, after heavy rain or recent flooding. Investigations of the soil moisture condition will be conducted based on experimentation.

The second physical condition of concern to the process of testing soil-gas radon is the temperature effect. The only established method for testing soil gas is based on mechanical introduction of soil gas which is drawn from the soil and into a scintillation cell while measuring the radioactivity of the gas based on alpha decay.

The possible effect of temperature can occur due to a temperature difference between the collection cell and the soil. This temperature difference may affect the flow rate upon which the soil gas is drawn and thus alter the device readings. Investigations of these conditions will be based on theoretical approach and supported by experimentation.

The third physical condition that might affect the testing process is similar to the one derived from temperature difference, that is, alteration to the flow rate

of the soil gas drawn from the system into the collection cell. This may develop from a pressure drop due to different lengths of tubing that might be used to conduct the test. Investigations of this pressure condition will be approached experimentally.

The fourth physical condition to address is soil compaction. Air flow through compact soil, as a part of the construction phase, may be affected by soil resistance to air flow. This determination depends on the soil compaction as an alteration to the soil's normal condition. Investigation of this approach will be done managerially.

Soil-Gas Radon Testing Methodology

Radon gas in the soil can be determined directly by testing its concentrations in soil gas. There are no federal or local standards for testing soil-gas radon in the soil. The most widely used procedure employs photomultiplier-based instrumentation to measure the decay of radon through alpha disintegration.

Soil-gas rich with radon is mechanically drawn into a scintillation cell internally coated with ZnS. The flow rate of the gas is controlled by a pump on the device. Soil-gas is drawn from the soil approximately two to four feet in depth by inserting a metal probe.

Before soil gas is introduced into the cell through tubing, it must be filtered from moisture and dirt or soil particles. Different types of filters can be used; however, the filter rating must be 0.8 micron to stop most radon progeny available in the soil gas.

Soil gas carrying radon and its progeny pass through the filter into the cell. If selected correctly, the filter stops radon progeny while allowing radon to pass into the scintillation cell. Soil gas pumping into the cell is applied for approximately ten minutes to allow for equilibrium between the radon concentration in the cell volume and the soil pore space. Pumping is stopped and then the cell is kept for a minimum of four hours before analysis. This period is necessary for radon within the cell volume to reach equilibrium with its progeny.

The cell is read by measuring the count per time unit interval using Pylon AB-5. Alpha particles, generated from radon and progeny decay inside the cell, strike the inner coating of film and generate lights. These light pulses are counted by a photomultiplier system through a photo-coupling fitted between the cell and the photomultiplier.

Pylon AB-5 is designed to provide the count, per any selected time interval, and incorporate the balance between the flow rate into the cell and the cell volume. The count rate (CPM) is then converted into a concentration (pCi/l) using a calibration factor. Figure 2-1 shows an

illustration of the soil-gas radon testing system using the Pylon AB-5 system.

Design of the Testing Chamber

Figure 2-2 illustrates the block diagram of the experimental assembly designed and constructed in this work. Design objectives taken into consideration include facilitating experiments mainly to investigate the effect of the first physical condition on the soil-gas testing process. Soil parameters such as permeability might have an effect on radon transport and thus should be minimized to isolate soil moisture as the control component. From a system standpoint, utilizing this assembly is intended for investigating soil moisture effects on radon availability in the soil, within the context of the soil-gas testing procedure.

The design incorporates a space for soil samples in which the effect of soil permeability is minimized by reducing the sample width. Radon generated from the sample is observed when the sample is subjected to a range of moisture. Soil samples are selected to place on a wide, open-face pan with a soil thickness of approximately 5 cm. This design is utilized to minimize the effect of soil permeability and spatial dependency of the radon diffusion

coefficient on the transport of radon from the soil sample into the chamber space.

The assembly is equipped with a differential pressure sensor, temperature sensor, and humidity sensor. A computer-controlled data acquisition system is utilized to collect the data on a continuous basis. The test chamber is connected to an adjacent chamber that houses the electronic equipment to detect soil-gas radon using scintillation cells. Air flow mechanisms, contributing to the convective transport of radon from the soil sample into the chamber space, were minimized by controlling temperature and pressure differences when possible. Temperature inside the chamber was kept the same as the room temperature to minimize temperature-driven air flow between the chamber and the outside.

An air leakage control valve was also used to compensate for conditions where convective flow may have occurred. Since the soil samples' surface area is large compared to the thickness, equilibrium between radon concentration in the soil pore space and the chamber space was considered to be reasonably achieved.

The design and conducting of experiments utilized a system approach in which comparative indicators are sought rather than absolute results. In this way, measurement of radon concentrations in the chamber space can represent, under the same operating conditions, the concentrations of

radon in the soil pore space. A change in the overall radon concentration in the soil pore space, therefore, is reflected in observed changes in the radon concentration measured in the assembly's chamber.

Design of the Experimental Procedure

In the testing chamber, radon gas collects due to the molecular diffusion process from the soil sample in the open pan into the equilibrium space. The space of the testing chamber was flushed with air prior to the start of each experiment. Radon concentrations were then continuously monitored to observe the buildup of radon gas in the chamber until reaching equilibrium inside the chamber. Radon concentration, pressure, temperature, and relative humidity data were simultaneously measured with a sampling time of 10 minutes, utilizing the data-logging system, and data were retrieved from the logging system into a personal computer system.

Soil samples were collected from three construction sites (representing typical construction soils in Florida) from three depths (2, 3, and 4 feet) typically representing the usual range where in-situ soil-gas radon measurements are performed. Soil samples were collected in sufficient quantities and placed into airtight containers (site containers), sealed, labeled, and transported to the

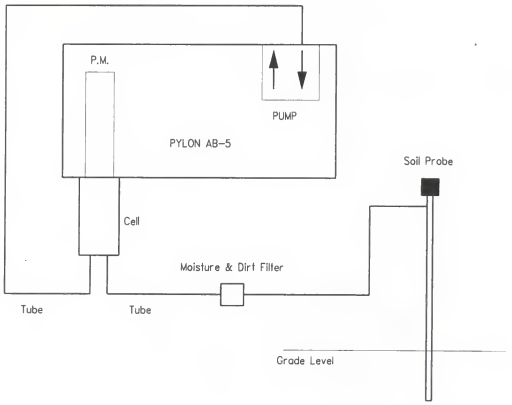

Figure 2-1: An illustration of the soil-gas radon testing system using photomultiplier-based instrumentation

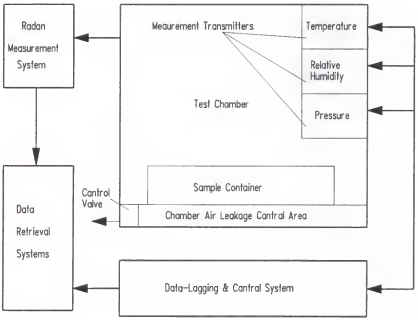

Figure 2-2: A block diagram illustrating the experimental assembly used to test the effects of soil water content on soil-gas radon measurements

testing laboratory.

At the lab, contents of site containers were divided into three parts; each was placed in a smaller airtight plastic container (lab container), and soil moisture was measured. Drying samples were prepared using a convectional hot-air oven for a minimum period of 48 hours. Dried samples were then placed in the lab containers, sealed, labeled, and left for a minimum of 14 days prior to testing to allow for radon to reach equilibrium with its parent. Saturated samples were prepared by adding water to soil samples until saturation.

Design of Pressure Measurements

Continuous measurements were designed to measure the time for dependent responses of pressure in the test chamber. Measurements were facilitated by using a standard 3/16-inch inner diameter metal tube which connects to the center of the test chamber. The tube is fitted into one port of a Setra (Model C264) differential pressure transmitter via plastic tube. The other port of the transmitter is left open. The transmitter is located outside the test chamber and placed in a closet which opens to the room where the testing assembly is housed.

The transmitter selected for this application is a very sensitive current-output differential-pressure transmitter

device which provides reasonable detection to the ranges of pressure differentials encountered in the experiments. The transmitter operates with a full-scale range of ±25 Pa and has a minimum sensitivity of less than 1% (±0.25 Pa); it provides a current control regulating to output signal to the industrial standard current of 4-20 mA.

The low-pressure port was left open to the room pressure. Therefore, the indoor pressure was used as the reference pressure. Since the transmitter operates in differential mode, its calibrated operating point is located at 12 mA. The transmitter then decreases the current flow if the pressure on the low port is higher than the pressure on the high port and vice versa. Figure 2-3 illustrates the operating range of the pressure transmitter and the linear equation used during data processing and calibration.

Transmitter current output is collected by the analog voltage input channel on the data acquisition and control system (Campbell Scientific 21X). Since the data input channel is for voltage, the transmitter current output was converted into voltage by using high-precision <1% shunt resistors. The pressure transmitter was zero-checked at the beginning of each experimental period and calibrated monthly according to the procedure described in a later section.

Design of Temperature and Humidity Measurements

Temperature and relative humidity were continuously monitored in the test chamber using Vaisala relative humidity and temperature transmitters (Model HMW 30 UB/YB). Temperature measurement utilized T-type (copper vs. copper-nickel) thermocouple wire and temperature transducer. This type of thermocouple wire was selected because of its resistance to humidity (bare wire) and the linearity between the signal output and the temperature degree for low-temperature ranges such as those encountered in these experiments. T-type thermocouple wire can be used to measure temperature ranges from -200 to 350°C (-328 to 662°F) on thermocouple grade and from -60 to 100°C (-76 to 212°F) on extension grade.

The relative humidity sensor of the transmitter achieves high accuracy in humidity measurement by sensing a capacitance change in a micron-thin polymer layer as it absorbs water vapor. This polymer is also unaffected by most dust and chemicals that might exist in the test-chamber environment. Both temperature and relative humidity sensors and associated circuits regulate the current in their corresponding power supply circuits to the standard output of 4-20 mA.

These signals are integrated into analog input voltage channels of the data acquisition and control system through

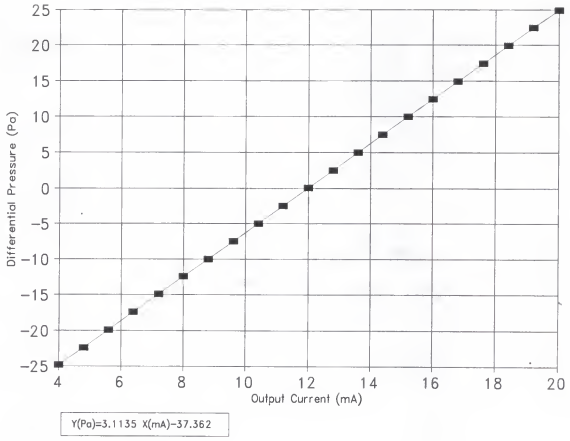

Figure 2-3: The linear correlation and operating range of the pressure measurement at the test chamber

high-accuracy shunt resistors. Figures 2-4 and 2-5 illustrate the operating range of relative humidity and temperature transmitters and show the linear equations used to calculate the equivalent engineering quantities from the reported output converted signals.

Design of Data Collection

For data logging purposes, the Campbell Scientific programmable micrologger (Model 21X) was utilized. One differential-mode analog voltage channel was used to log the pressure differential signals, and two single-mode analog voltage input channels were used for the temperature and relative humidity signals.

The logging and control system is equipped with standard Programmable Read-Only Memory (PROM) that is used for the system's operational programs. The system supports eight analog input channels, four pulse input channels, four excitation output channels, two continuous analog output channels, and six digital control ports. It can be remotely operated, and it supports standard serial input/output communications.

The system is programmed with a group of command instructions entered into a program table which can be executed according to a pre-specified execution interval. The latter interval determined the minimum time that

measurements controlled by the system and data collection could be performed. The data in the system were periodically retrieved through a phone line into a personal computer at the Department of Civil Engineering.

Design of Soil-Gas Radon Measurements

The experiments consisted of measuring radon gas in the test chamber corresponding to the tested soil samples. Radon measurements were designed to monitor radon concentrations continuously in order to characterize both transient and steady-state responses due to the specific soil-gas radon diffusion from the soil samples.

Continuous time-dependent measurements of radon concentrations in the test chamber were performed using a Pylon (Model AB-5) portable radon-monitoring system obtained from the Department of Nuclear and Radiological Engineering. Soil-gas radon measurements in the test chamber were performed simultaneously with other measurements of temperature, pressure, and relative humidity for each of the tested samples.

Pylon AB-5 is a portable, programmable microprocessor-based data-acquisition photomultiplier radiation monitor equipped with modular accessories that can be used for measuring radon and thoron gas, airborne alpha particles,

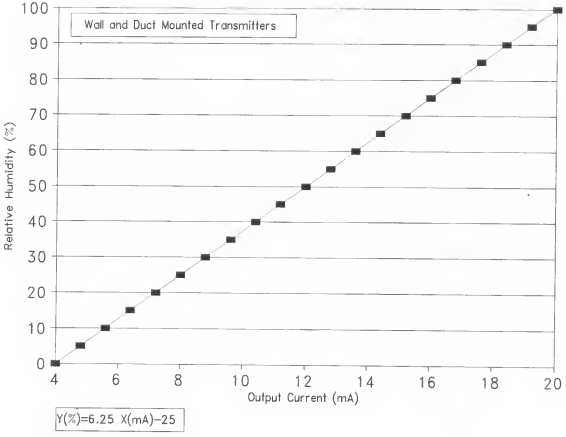

Figure 2-4: The linear correlation and operating range of the relative humidity measurement at the test chamber

beta and gamma radiations, and surface contamination. However, in this application, only airborne radon measurement was needed. To facilitate measurement of radon in the test chamber, soil gas was allowed to diffuse directly to the measurement cell via a 1-foot flexible duct sealed to the test chamber. Passive Radon Detector cells (Model PRD-1) were used. Measurements using these cells were performed by allowing the soil gas to diffuse through the flexible duct and into the cell volume.

An equilibrium time of approximately one hour is required for the PRD cell volume to achieve the same radon concentration as the gas level present in the test chamber. The cell is lined with ZnS(Ag) scintillator material on the internal metal surface. Light pulses are generated when the alpha particles emitted from radon strike the scintillator surface. The cell is fitted to a photomultiplier window coupler, where generated pulses are collected and computed. The cells were flushed with room air and measured for radon residual upon the conclusion of each test run.

The Pylon counts were accumulated over 10-minute intervals, stored in the monitor memory at the end of each interval, and then downloaded to an IBM PC at the end of the experiment period. Experimental periods of various lengths, but typically 72 hours, were used to perform the measurements. This period provided information on the soil-

gas radon response during the transient period as well as after the test chamber system had stabilized.

Collection and Processing of the Experimental Raw Data

To ensure the quality of the experimental data and the data analysis collection, the processing and classifying of the raw data and the calibration processes were carefully conducted. At the conclusion of each experimental run, two groups of output data files were generated.

The first group logs the Pylon cycle run and the soil-gas radon concentration data. The second group logs the experiment run time, temperature, relative humidity, and differential pressure data. Raw data logged into the two groups' files were retrieved into a BASIC program and rewritten as processed data files in ASCII format.

Modifications to the raw data included calculations of the equivalent engineering value corresponding to the collected voltage according to the calibration curve of the particular instrument. Processed data files were assigned names indicating the experimental run number and dates and kept consistent during the period of this research.

The processed ASCII files were then imported into a spreadsheet software (QuattroPro) for plotting, exchange, and analysis purposes. The name structure of each processed ASCII file is kept the same with the exception of changing

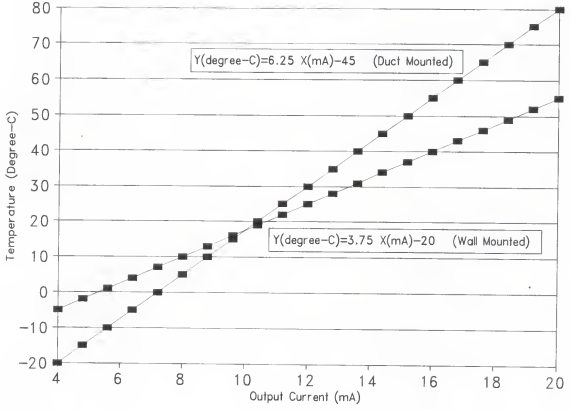

Figure 2-5: The linear correlation and the operating range of the temperature measurements at the test chamber

the file extension from (.PRO) to (.WQ1) while stored in the spreadsheet format.

Design of Tube-Length Effect Experiments

Under the physical condition of pressure discussed earlier in this chapter, pressure drop resulted. Different tube lengths to draw soil gas into the testing system (Figure 2-1) might have an effect on the representation of soil-gas radon concentration. An experimental setup was developed to observe and verify whether tube length adversely affected measured radon concentration and thus contributed to a misrepresentation of soil-gas radon.

Figure 2-6 provides an illustration of the experimental setup utilized for the purpose of investigating tube-length effect on soil-gas testing following the typical soil-gas testing procedure outlined earlier. The testing setup consisted of a Pylon AB-5 portable radiation monitor, a Lucas scintillation cells (Model 300), plastic tubing at different lengths, and a radon source.

A drum, half-filled with radium-based paint peeled from old military airplanes, was used as the radon source. The drum was prepared and calibrated at the Department of Nuclear and Radiological Engineering (NRE).

Testing was performed using four scintillation cells calibrated by NRE. The four cells were flushed with fresh air upon the conclusion of each experimental run and checked before the next run was prepared.

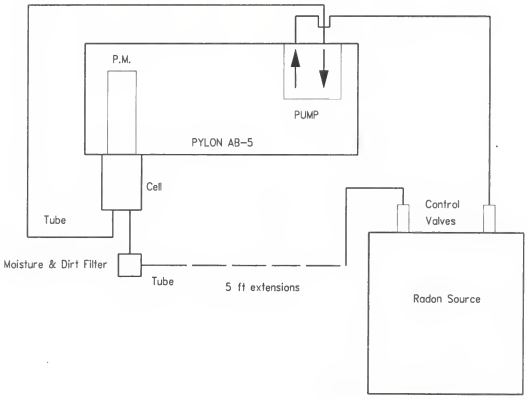

Figure 2-6: An illustration of the experimental setup to investigate tube-length effect on soil-gas radon testing

Tube lengths were varied on 5-foot segments. Testing was performed for each 5-foot tube segment sequentially. A period of 5 minutes was utilized to circulate the air through the scintillation cell before collecting the sample.

Once the sample was collected, tube length was changed and the procedure repeated using another cell. Cells were labeled, kept for a minimum of 4 hours, and then measured using pylon AB-5. Radon concentrations were obtained from measuring the count rate, accounting for the correction that resulted from radon decay, and employing the calibration factors developed by NRE. The same pumping system (Pylon AB-5) was used to draw the samples.

Average radon concentration per each five feet segment of tube length was compared to each other and the reference radon concentration in the drum. The latter was calibrated by NRE using a combination of passive and active radon measurement instrumentation.

Quality Control and Assurance

A quality control and quality assurance plan was utilized during the execution of this research. Procedures of calibrating devices and equipment used for performing the measurements were followed and implemented. Data representations were performed through assessment of the

potential experimental errors associated with the measurements.

Human and system errors form a significant part of errors associated with experimental data. Human-related errors are generated from the experiment conductor's activity that may cause the system to malfunction or cause an error during data collection, processing, analysis, and/or interpretation. System errors are generated because no system is perfect and from uncertainties developed by the distribution of the variable being tested.

Minimization of system errors was implemented by applying and following a careful design of the experimental setup, including selecting instrumentation, performing continuous equipment calibration as often as needed, and cross-checking experimental results for different types of devices that measure the same parameter. Minimization of human errors was achieved by performing the experiment carefully and also by repeating the testing.

In most physical measurements, error estimates can be used to evaluate the overall system performance with regard to the accuracy of the measurements and associated error calculations. The estimators applied in the assessment process are the following (Al-Ahmady 1995):

(1) Hysteresis is the maximum difference in the system signal output, at any measured value within the specified

range, when the value is approached first when increasing and then decreasing the variable under measurement.

(2) Linearity is the maximum deviation of any calibrated point on a specified straight line (representing the best straight line fit), during any one calibration cycle.

(3) Repeatability is the ability to reproduce output readings when the same variable under measurement is applied consecutively, under the same conditions, and in the same direction.

(4) Thermal error is the maximum change in output, at any value of the measured variable within the specified range, when the temperature is changed from room temperature to a specified temperature extreme.

(5) Thermal zero shift is zero shift due to changes of the ambient temperature from room temperature to the specified limits of the operating temperature range.

(6) Overall thermal error is the combined error of thermal zero shift and thermal error calculated using the root sum of the squares (RSS) statistical method.

(7) Accuracy is the combined error of repeatability, hysteresis, and linearity calculated using the RSS method.

(8) Overall combined error is the combination of all the previous possible errors, when applicable, calculated by using the RSS method.

Calculation of the overall experimental error is computed using the statistical RSS method. Most of the equipment used during this research had inherent hardware corrections to the errors in their output signals that resulted from thermal- driven factors. Such inherent corrections may cause changes to applied correction levels of approximately 70-100 % of the device output signals, depending on the particular instrument and the condition of the experiment.

However, in the following assessment of the overall experimental error, the maximum possible overall thermal error (OTE) was used in the computation, resulting in a 0% correction level consideration from the instrument-inherent corrections. Therefore, the utilized assessment is considered conservative by implementing a built-in safety consideration of 0% thermal correction on the part of OTE, and by using the maximum possible error that might be driven from non-linearity, non-repeatability, and hysteresis factors for computing the combined accuracy error (CAE).

The assessment criteria developed to compute the overall combined experimental error (OCEE) associated with the measurements performed during this research is

$$OCEE = [OTE^2 + CAE^2 + OSE^2]^{0.5}$$

where OSE represents all other possible sources of system error that are individually based on particular instrumentation and/or particular applications such as

errors induced by fluctuations of the external power supply voltage.

Errors associated with differential pressure measurement are those of the Setra C264 pressure transmitters. The first system error which may occur is overall thermal error. This is associated with the Setra C264 ($\leq \pm$ 0.0033 %) from the full scale (FS) per each temperature degree difference from the factory-adjusted calibration temperature of 21.1 °C (70 °F). The range of temperatures at which experiments were performed during this research was -1.1 to 37.78 °C (30 to 100°F), giving a maximum temperature difference of 4.45 °C (40 °F) from the factory-adjusted temperature. This difference results in a maximum overall temperature-induced error (TIE) of (0.0033% FS/degree x 40 °F = 0.132 % FS) in the transmitter output signal.

The transmitter has an infinite resolution factor and repeatability factor of < 0.3% FS. The combined RSS statistical accuracy error (CAE) value of the system is $\leq \pm$1.0% of the full scale. Since the C264 transmitter regulates current rather than voltage as an output signal, its circuit current may be introduced with an error resulting from variations in the power supply voltage. This error corresponds to a 0.02 mA change in the transmitter's current output, per volt change in the power supply.

The transmitter was calibrated for both zero and span adjustments. The standard calibration procedure is used for zero adjustment by applying a factory-selected 24 volts from a power supply (by voltmeter) and a 250-ohm load for the shunt resistor on the 21X data-acquisition system. The output current was adjusted to 12 mA, the operating point for these measurements, for bi-directional range from the zero adjustment screw in the transmitter, when both pressure ports are connected by a flexible tube.

Temperature measurements performed by the Vaisala HMW 30UB/YB transmitter have a linearity error factor of <0.1°C, and an overall thermal error of ±0.02°C. The overall accuracy factor of the system is ±0.2°C. Utilizing the same upper end temperature of 37.78°C (100°F), the resultant maximum uncertainty in the signal output due to the thermal zero shift and thermal errors is 0.75°C. Therefore, the overall combined experimental error associated with these temperature measurements is <±0.78°C.

The output signal for the relative humidity has an overall thermal error factor of ±0.04% FS/°C. An overall accuracy, including linearity and repeatability factors, of ±2% FS for a relative humidity range of 0-90% and ±3% for a relative humidity range of 90-100%. Since the maximum possible measurement error developed by temperature is ±1.508% FS, the maximum combined experimental error of the relative humidity measurements is <±2.5% FS for a relative

humidity range from zero to 90%, and <±3.6% FS for a relative humidity range of 90-100%.

Quality control of the soil-gas radon measurements conducted in this research was ensured by the calibration activity of the Pylon AB-5. The device was regularly calibrated at the Department of Nuclear and Radiological Engineering through the participation in the United States Department of Energy Environmental Measurement Laboratory (EML) calibration activities (Al-Ahmady 1995).

CHAPTER 3
RESULTS AND DISCUSSION

Observation and Evaluation of the Testing Configuration Condition

As outlined in the Scope of Methodology section of Chapter 2, when the components of the soil-gas radon testing process are considered (in validating the test results to facilitate the management decision), testing configuration is one of the four conditions that must be investigated.

The most widely used testing configuration available is the utilization of scintillation cells and radiation instrumentation to measure alpha decay generated from radon in the soil gas. This methodology is discussed in the Soil-Gas Radon Testing Methodology section of Chapter 2.

Figure 2-1 illustrates the most widely used experimental setup for the purpose of testing soil-gas radon concentrations. Within this setup, testing configurations are relatively limited. However, the most possible variations are changes in the length of the tubing. Due to construction site characteristics, testers have been using different lengths of tubing to complete the test in the easiest way. The test may be performed according to the availability of tubing at the

site, surface water in the site, availability of shelter, and availability of electric power.

For the purpose of this research, the likelihood that a tester will change the test configuration is mainly restricted to the use of different tubing lengths. Accordingly, results should be viewed and used within this scope. Pressure is defined as the most significant condition that might alter the validity of the results within the soil-gas testing configuration. Pressure condition alterations due to changes in the tubing lengths was investigated by utilizing the experimental assembly specifically designed for this purpose (Figure 2-6). Using this assembly, radon concentrations were drawn from the drum, which was considered a constant source representing the soil gas, and passed through tubing lengths ranging from 5 to 50 feet and segmented every 5 feet.

Tables 3-1, 3-2, 3-3, and 3-4 show the results of these measurements. To attain results from the scintillation cells, which were filled with sample gas drawn from the drum, the measurements in Table 3-1 were kept for 271, 296, and 408 minutes (a minimum of 4 hours) before accounting for tube lengths of 5, 10, and 15 feet, respectively. Samples collected for tubing lengths of 20, 25, and 30 feet were kept for 434, 308, and 276 minutes, respectively (Table 3-2).

Results of configurations of tubing lengths of 35, 40, and 45 feet are shown in Table 3-3. In these, the elapse time between the radon collection time and the measurement time was

Table 3-1: Results of the tubing length (5, 10, and 15 feet) effect on the measured radon concentration using the testing setup of Figure 2-6. (L = tube length, E.T. = elapse time, CPM = counts per minute, Rn-C = radon concentration in pCi/l)

L (ft)	5			10			15		
Cell no.	203			781			584		
E.T.	271			296			408		
	Min	CPM	Rn-C	Min	CPM	Rn-C	Min	CPM	Rn-C
1	272	262	189.7	297	254	182.3	409	288	179.8
2	275	269	155.2	269	243	171.5	410	233	147.2
3	276	284	177.5	269	297	167.3	411	238	147.2
4	275	275	171.0	300	254	177.2	412	227	143.4
5	276	254	156.9	301	288	187.1	413	229	144.7
6	277	297	179.5	302	288	201.3	411	214	135.2
7	276	269	162.0	308	231	163.1	415	189	119.4
8	275	269	168.2	308	269	180.8	411	230	145.4
9	280	269	165.8	308	238	166.7	417	215	139.8
10	288	308	180.8	308	288	172.4	410	269	129.6
11	262	308	192.7	307	252	178.1	411	269	129.6
12	263	297	180.8	308	242	171.0	411	181	114.4
13	280	269	186.5	309	238	168.2	411	222	140.4
14	288	254	159.0	314	252	206.4	412	208	130.3
15	286	288	155.2	311	227	160.5	411	232	146.8
16	297	275	174.7	312	269	160.2	411	195	123.4
17	288	288	167.8	313	231	163.3	415	221	139.8
18	289	297	160.5	314	254	179.6	415	214	136.7
19	280	273	171.0	315	288	187.1	417	219	139.8
20	231	288	177.9	314	288	180.8	415	192	121.5
21	292	277	173.5	317	255	180.4	419	240	151.9

Table 3-1 Cotinued

L (ft)	5			10			15		
Cell no.	203			781			584		
E.T.	271			296			408		
	Min	CPM	Rn-C	Min	CPM	Rn-C	Min	CPM	Rn-C
22	293	257	167.3	318	257	181.9	420	211	133.6
23	296	278	174.2	319	242	171.3	421	217	137.4
24	296	311	194.9	320	282	199.6	422	238	150.7
25	296	273	171.1	321	260	175.5	423	212	134.3
26	297	296	179.3	322	222	157.2	424	215	136.2
27	238	260	163.0	323	297	182.0	425	230	145.7
28	299	290	181.8	324	278	196.9	426	216	136.9
29	300	279	175.0	325	249	176.3	427	223	141.3
30	301	287	180.0	326	262	185.6	428	214	135.6
Avg.			173.7			179.0			138.5
Std. Dev.			10.99			12.09			11.84

313, 395, 431, and 457 minutes, respectively. The results for the 50-foot tube length are shown in Table 3-4.

The delay is necessary for allowing time to eliminate activity contributions from the radon progeny. These might have been present during the collection time. Despite filters being used in the tubing line, this is a normal means to remove most radon progeny present in the gas stream being tested.

Tables 3-3 and 3-4 show the results of the count rates

and the corresponding concentrations of radon found in the cells used with tube lengths of 30, 35, 40, 45, and 50 feet. The corresponding elapse time between the filling and counting were 276, 313, 395, 431, and 457 minutes, respectively.

Table 3-2: Results of the tubing-length (20, 25, and 30 feet) effect on the measured radon concentration using the testing setup of Figure 3-6 (L = tube length, E.T. = elapse time, CPM = counts per minute, Rn-C = radon concentration in pCi/l)

L (ft)	20			25			30		
Cell No.	596			720			203		
E.T.	434			308			276		
	Min	CPM	Rn-C	Min	CPM	Rn-C	Min	CPM	Rn-C
1	438	143	105.7	309	97	70.5	277	116	84.0
2	438	170	107.7	310	89	49.9	279	93	58.1
3	437	173	109.6	311	101	63.0	279	89	59.4
4	438	153	97.0	312	95	59.2	280	104	65.0
5	439	150	95.1	310	119	74.2	281	116	71.3
6	440	140	88.7	310	92	97.0	282	108	67.5
7	444	160	101.4	315	89	55.5	283	89	53.2
8	442	150	109.6	310	108	67.4	280	94	58.8
9	443	101	89.4	317	105	65.5	285	78	48.8
10	444	150	97.7	310	94	88.7	286	89	55.7
11	445	163	103.4	319	81	50.5	287	105	65.7
L (ft)	20			25			30		
Cell No.	596			720			203		
E.T.	434			308			276		

Table 3-2 Continued

	Min	CPM	Rn-C	Min	CPM	Rn-C	Min	CPM	Rn-C
12	448	145	93.9	326	110	68.7	288	80	50.7
13	447	159	100.9	321	91	96.6	288	104	62.6
14	448	159	100.9	322	95	59.3	290	109	68.2
15	440	138	87.6	326	102	68.7	291	87	54.5
16	453	151	96.6	326	109	68.1	292	81	50.7
17	451	145	92.0	326	106	66.2	293	87	54.5
18	452	141	89.5	326	80	52.5	294	82	51.3
19	453	141	102.2	327	102	68.7	295	109	68.3
20	440	159	101.0	326	104	65.0	296	102	63.9
21	453	145	100.9	329	102	68.7	297	113	70.8
22	453	131	83.2	330	102	68.7	298	87	54.5
23	457	152	96.6	331	98	60.3	293	109	69.8
24	448	177	112.5	332	97	60.6	304	104	65.2
25	453	152	96.6	333	80	96.6	304	102	63.9
26	440	148	96.6	330	88	65.0	302	114	71.5
27	461	162	103.0	335	80	52.5	303	91	57.1
28	452	145	94.7	330	87	41.9	304	104	65.2
29	453	145	94.7	337	92	57.5	305	110	69.0
30	464	156	99.2	330	112	70.1	304	107	67.1
Avg.			98.03			60.45			62.08
Std. Dev.			6.66			7.23			7.89

Counting procedures follow the practice established by the NRE during the counting by taking 30 readings, correcting for the time difference in radon decay, and using calibration factors to convert Pylon AB-5 count-per-minute (CPM) readings

into concentration units. Radon concentrations in each cell, corresponding to a specific length of tubing in these experiments, are the simple average of the 30 corrected readings of that cell. The simple average and corresponding standard deviation for the tests of 5 to 50 feet in 5-foot segments are given in Tables 3-1 and 3-2.

Table 3-3: Results of the tubing-length (35, 40, and 45 feet) effect on the measured radon concentration using the testing setup of Figure 3-6 (L = tube length, E.T. = elapse time, CPM = counts per minute, Rn-C = radon concentration in pCi/l)

L (ft)	35			40			45		
Cell No.	781			584			596		
E.T.	313			395			431		
	Min	CPM	Rn-C	Min	CPM	Rn-C	Min	CPM	Rn-C
1	314	55	40.0	396	48	35.3	432	54	39.9
2	315	52	36.7	397	67	42.2	433	45	28.5
3	316	54	45.2	398	56	36.5	434	51	32.3
4	317	54	38.2	399	54	40.8	435	52	32.9
5	319	71	50.2	400	56	36.6	436	52	36.7
6	319	69	48.8	401	61	38.4	437	52	32.9
7	320	45	31.8	402	53	33.4	438	42	26.6
L(ft)	35			40			45		
Cell	781			584			596		
E.T.	319			399			434		
	Min	CPM	Rn-C	Min	CPM	Rn-C	Min	CPM	Rn-C
8	321	43	30.4	403	67	42.2	439	53	33.6
9	322	55	38.9	404	72	45.4	440	34	21.5

Table 3-3 Continued

10	323	43	30.4	405	69	43.5	441	47	29.8
11	324	52	36.8	406	77	48.6	442	55	34.8
12	325	57	40.3	407	56	35.3	443	44	27.9
13	326	51	36.1	408	50	31.5	444	53	33.6
14	327	44	31.1	409	53	33.4	445	42	26.6
15	328	67	47.4	410	65	41.0	446	50	31.7
16	329	66	46.7	411	60	37.9	447	55	34.9
17	330	51	36.1	412	57	36.0	448	53	33.6
18	331	61	43.2	413	60	37.9	449	43	27.3
19	332	49	34.7	414	68	42.9	450	61	38.7
20	333	64	45.3	415	49	30.9	451	49	31.1
21	334	55	39.0	416	45	28.4	452	53	33.6
22	335	62	43.9	417	48	30.3	453	63	40.0
23	336	54	38.3	418	58	36.6	454	48	30.4
24	337	53	37.6	419	74	46.8	455	58	36.8
25	338	53	37.6	420	57	36.0	456	61	38.7
26	339	63	44.7	421	63	39.8	457	47	29.8
27	340	47	33.3	422	72	45.5	458	46	29.2
28	341	53	37.6	423	57	36.0	459	53	33.6
29	342	63	44.7	424	61	38.6	460	50	31.7
30	343	45	31.9	425	58	36.7	461	56	35.6
Avg.			39.2			38.18			32.5
Std. Dev.			5.59			4.93			4.24

Table 3-4: Results of the 50-foot tube-length effect on the measured radon concentration using the testing setup of Figure 3-6 (L = tube length, E.T. = elapse time, CPM = counts per minute, Rn-C = radon concentration in pCi/l)

L (ft)	50								
Cell No.	720								
E.T.	457								
	Min	CPM	Rn-C	Min	CPM	Rn-C	Min	CPM	Rn-C
1	458	44	32.6	468	33	21.0	478	36	22.9
2	459	31	19.7	469	46	29.2	479	35	22.3
3	460	48	30.5	470	31	19.7	480	36	22.9
4	461	31	19.7	471	45	28.6	481	33	21.0
5	462	35	22.2	472	38	24.2	482	43	27.4
6	463	38	24.1	473	53	33.7	483	40	25.5
7	464	35	22.2	474	50	31.8	484	46	29.3
8	465	45	28.6	475	48	30.5	485	37	23.6
9	466	37	23.5	476	40	25.4	486	34	21.6
10	467	49	31.1	477	47	29.9	487	40	25.5
Avg.									25.71
Std. Dev.									4.18

Observation of the average radon concentrations for the experimental runs correspond to tube lengths from 5 to 50 feet. This indicates that obtained concentrations are decreasing as the tube length increases. This observation is significant in terms of validating the condition of the experimental setup to test for soil-gas concentration, as a

potential indicator to the need to incorporate a passive or active radon-control system decision prior to construction.

Figure 3-1 illustrates a bar diagram plot of the average radon concentration versus the length of the tube. As seen in the plot, obtained concentrations dropped from approximately 174 pCi/l to 26 pCi/l when the tube lengths used were 5 and 50 feet, respectively. This is a drop of approximately 7 times and is very substantial in underestimating the soil-gas radon concentration.

The effect of the tube length may easily alter the management decision in determining the need to install a radon-control system from positive to negative. At a tube length of 20 feet, radon concentration dropped by more than half (approximately 56%) compared to the obtained concentration at the tube length of 5 feet, although the source of radon is the same. Figure 3-1 also shows the standard deviation of the average radon concentrations obtained from these experiments.

The standard deviation for each experimental run corresponding to a tube length is plotted at the top of the bar drawing representing the average radon concentration. Calculated standard deviations were performed based on the 30 decay-corrected radon concentration readings of the grab samples collected in this experiments.

The general trend of the standard deviation is consistent with the calculated average radon concentrations. Fluctuations in the calculated values are derived from the

radon nature of the radioactive decay of radon gas in the testing cells. Consistency was observed throughout the samples, as the absolute value of the standard deviation generally decreases with the decrease in the corresponding average radon concentration.

To better assess the relationship of the range of fluctuation associated with each tube experiment, the ratio of the absolute value of the standard deviation to the corresponding average indoor radon concentration is plotted in Figure 3-2. The ratios, expressed in percentages, reflect the statistical uncertainty in the measured and calculated average radon concentrations.

As seen in the graph, the maximum statistical uncertainty is less than 20%. Uncertainty gradually increased by increasing the tube length, which is a normal observation when the number of events, corresponding to the decay of radon in the test cell, becomes smaller as the length of the collection tube increases. The range of statistical uncertainty is acceptable within the scope of such measurements.

Figure 3-3 shows the plot of the experimental values of average radon concentration versus the tube length. A clear exponential relationship is shown in the graph. An exponential curve is fitted to the data where the dependent variable (Y) is assigned to the average radon concentration and the independent variable (X) is assigned to the collection tube length. The best-fitted curve provides an exponent coefficient of 0.0464 and an initial average radon

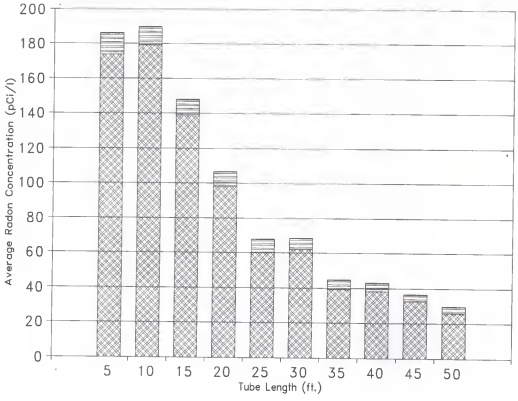

Figure 3-1: Average radon concentrations as a function of the soil-gas radon collection tube (or line) and the corresponding standard deviations

concentration of approximately 242 in the following form:

$$Y\ (pCi/l) = 242.26 \exp [-0.0464\ X\ (feet)]$$

The initial average radon concentration that corresponds to a zero tube length is obtained from the above equation when X takes the value of zero. Figure 3-3 also shows the exponential relationship between the average radon concentration and the length of the collection tube in the experimental setup of Figure 3-6.

Errors associated with the above fitted equation can be assessed from calculating the average square root of the square of difference between the equation value and the experimental value for a given length. Figure 3-4 shows the square root value of the square of difference between the experimental average radon concentration and the predicted average radon concentration using the above equation for tube lengths from 5 to 50 feet. The average root square value of the square of differences between the experimental and mathematical average radon concentrations is approximately 13 pCi/l.

The above results indicate that the experimental configuration condition and specifically the length of the tube used to collect soil gas during the testing of soil-gas radon concentration can adversely affect the reported concentrations. This is the main measurement figure that a construction manager would use to complete the decision to incorporate a radon-control system into building construction plans. Therefore, the soil-gas system configuration must be

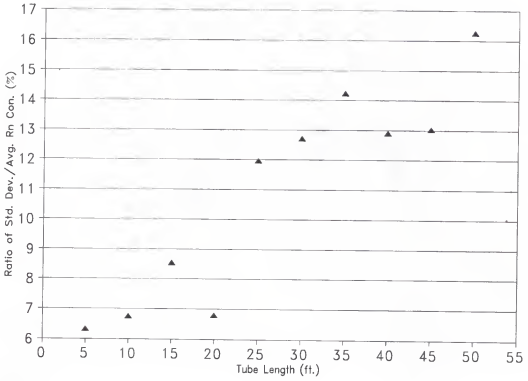

Figure 3-2: The maximum percentage of average radon concentrations that is attributed to statistical uncertainty of the measurement

carefully considered. Using the above equation, the theoretical average radon concentration at no tube length is the same as the coefficient in the equation when the length variable is set to zero. Therefore, the effect of the length of the collection tube or line on the measured soil-gas concentration can be assessed from

$$Y/Y_o = \exp [-0.0464 X]$$

where Y_o is the theoretical zero-tube-length average radon concentration. Figure 3-5 shows the relationship between the reduction in average radon concentration and the tube length. According to this figure, a collection tube length of more than 50 feet may result in affecting the reported soil-gas concentration by more than 90% lower than the concentration immediately available in the soil.

An explanation for this observation can be derived from the relationship between the pressure drop across the collection pump and the collection time. Soil-gas samples are collected in the scintillation cells in preparation for measurement at a later time to correct for the decay of radon progeny. The collection procedure involves circulation of soil gas throughout the scintillation cell to obtain a representative sample (Figure 2-6). Most of the pumps used for this type of measurement are built into the system of measurement (for example, the Pylon AB-5). This is designed to provide a maximum air flow rate of 4 liters per minute (l/m) under zero static pressure. Most similar built-in pumps are designed to operate within the range of 0.5 to 4 l/m under

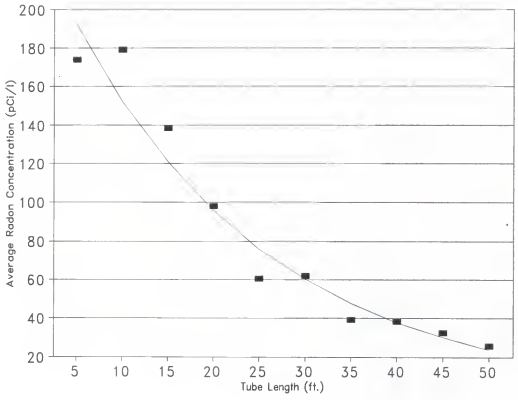

Figure 3-3: Experimental and fitted relationships between the average radon concentration and the length of radon collection tube of the soil-gas radon testing setup

zero static pressure and typically adjusted to 1.8 to 2 l/m.

The subsoil system where soil-gas samples are drawn represent a substantial resistance to air flow, especially in low-permeability soils and fill materials, compared to air drawn from the outdoors or indoors. The adverse effect of the lengthy collection tube or line is attributed to two factors: (1) mass flow rate is changing due to the length of tube; and (2) the length of tube is contributing fresh air into the cell in which the soil-gas sample is misrepresented. This is strongly dependent upon the collection time.

A collection time of 5 or 10 minutes under a specific pressure drop associated with a 5-foot collection tube would probably allow enough soil gas to be drawn into the cell (in which the cell volume is in equilibrium with the soil gas). However, the same collection time of 5 or 10 minutes may not be sufficient to bring enough soil gas through a lengthier collection tube at the lower flow rate in the system.

Further, more fresh air would have to be removed (in a longer tube) before soil gas reached the cell. If the collection time is not sufficient, the content of the system scintillation cell volume is not representative of the soil gas. This results in a configuration with lower radon content, in turn resulting in a lower radon concentration when samples are measured after the 4-hour waiting period.

The procedure to test for soil-gas radon concentration prior to construction as a potential for indoor radon problems must consider the compatibility of the radon collection tube

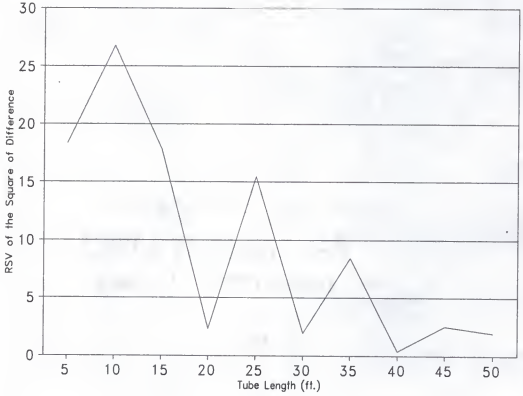

Figure 3-4: The square root of the square of difference between the experimental average radon concentration, and the predicted average radon concentration as a function of the collection tube length

and sample collection time.

It is suggested that counts be monitored during the collection of the soil-gas sample. Most electronic instrumentation, such as Pylon AB-5, permits a count during the sniffing. This does not interface with the soil-gas flow rate into the pump. The user should then establish a plateau from the sniff count before collecting the grab sample. This will ensure that a representative sample is obtained and will minimize adverse effects of the testing configuration conditions on soil-gas radon testing.

Observation and Evaluation of the Temperature Condition

Temperature effects on the testing of soil-radon gas concentration prior to construction are expected to have an indirect effect. The latter may be developed from different temperatures between the site soil and the testing cell used during the test. Temperature of the soil-gas at depths of 2 to 4 feet, where soil gas is typically drawn for the purpose of the soil-gas radon testing, is not a parameter under the tester's control. A general framework is needed to address the temperature effect. The framework should relate between the temperature in a first region (the soil) and the temperature at a second region (the scintillation cell). The indirect effect of temperature differences between the first and second region may be developed by altering the differential pressure normally generated between the two

regions and associated with the flow of soil gas from the soil pore space into the testing cell. Thus, to investigate such an effect, a general model was employed that can relate temperature differences to corresponding pressure differences between two regions (or areas) that are relatively separated.

The temperature-induced pressure differential model was developed by Al-Ahmady (1995) for applications concerned with indoor radon concentration driving forces and the design and optimization of radon control systems. Although the application for which the model was developed differs from this application, the model is readily applicable to any two zones that exhibit different temperatures. For the purpose of providing the general analytical basis for the model development and the integrity of information provided in this research, the temperature-induced pressure differential model is re-derived in this work. The analytical approach to developing the temperature-induced pressure differences can be achieved by employing the fundamental physics concept of the conservation of forces related to pressure under hydrostatic equilibrium. If pressure in the specific zone is under hydrostatic equilibrium, the forces with air pressure must counteract the gravitational force.

If a specific volume is considered under such equilibrium, the net force at any point in this volume must be zero; therefore,

$$dP/dh=-\rho g \qquad (3\text{-}1)$$

where h is the height measured from a reference level (m),

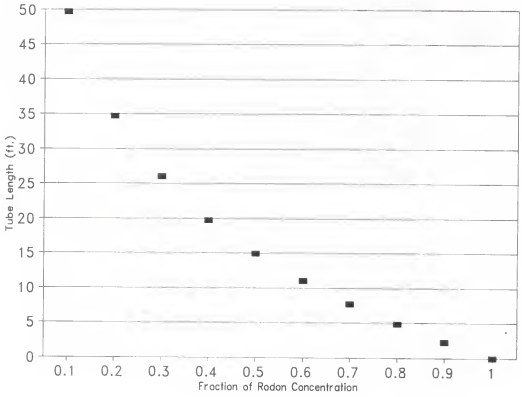

Figure 3-5: Ratio of measured average radon concentration to zero-tube radon concentration per length of the collection tube

ρ is the air density (kg/m^3), and g is the gravitational acceleration constant ($9.8\ m/s^2$).

Air can be considered an ideal gas for this application. Thus the ideal gas law may be used to introduce the temperature into the above equation, through the equivalent of the right-hand side of Equation 3-1, ρg as

$$dP/dh=-P(mg/kT) \qquad (3\text{-}2)$$

where m is the mass of air (kg), k is the Boltzmann constant (1.38×10^{-23} J/K), and T is the absolute temperature (K).

Equation 3-2 establishes the explicit relation between temperature and pressure in a specific volume representing a zone in this application; however, this relation is not linear, as will be shown by its solution. An analytical solution to this first-order differential equation requires application of a boundary condition.

An applicable boundary condition to this implementation is $P=P_o$ at $h=0$, which yields

$$P=P_o \exp(-mgh/kT) \qquad (4\text{-}3)$$

The location of the soil-gas radon testing system (one temperature zone) is usually near the ground surface, however, to account for possible usage, a maximum height of approximately 4.5 feet above the ground can be safely selected. It is highly unexpected that the testing assembly will be placed at heights more than a foot or two from the ground.

Utilizing the maximum height selection (1.4 meters), the

magnitude of the quantity (mgh/k) represents a constant of value C=0.0477 K, when m is the average molecular mass of air (28.8 u) at an atmospheric composition of approximately 80% N_2 and 20% O_2, at uniform temperature of 280 K.

Because the constant C is small, the value of the exponent on the right-hand side of Equation 3-3, exp(-C/T), is approximately unity and can be approximated as (1-C/T). Applying this treatment to two pressure conditions P_1 and P_2, which correspond to temperatures T_1 and T_2, respectively, yields

$$P_1-P_2 = \Delta P = P_o\ C\ [(T_1-T_2)/T_1T_2] \qquad (4-4)$$

the pressure difference generated between two zones of different temperatures. This equation can be used to characterize the pressure differences induced by soil-gas zone temperature (temperature of the soil gas in the soil pore) and soil-gas testing cell zone (temperature inside the testing cell).

A simpler analytical format that linearly relates the pressure differentials between two zones developed from different zone temperatures is that developed by Furrer et al. (1991). According to Furrer's model, the relationship between differential pressure and differential temperature can be written as

$$\Delta P = \Delta T \times k \times g \times h \qquad (4-5)$$

where ΔP is the pressure difference in pascal developed due to temperature difference, ΔT in °C, k is a constant representing the specific decrease in air density ($4x10^{-3}kg/m^3K$),

g is the acceleration due to gravity (9.8 m/s^2), and
h is the height above the basement level (m).

If the same height of 1.4m is used in this model, Furrer's and Al-Ahmady's models are in agreement within 15%.

The temperature-induced pressure differential model can be used to predict pressure differences induced over a range of temperature differences. Figure 3-6 shows predictions of the temperature-induced pressure differences over a temperature difference ranging from -50 to 50°K.

As seen in the graph, the temperature-induced pressure differentials show a linear relationship with the temperature-difference driving forces. Differences between the indoors (inside the testing chamber) and outdoors (inside the room where the assembly is located) show a linear correlation with the corresponding temperature differences.

Temperature differs between the soil zone (or area) where the soil-gas radon testing tube is located and the testing cell, where the difference is not expected to be large. Although no experiments were conducted in the field, unless the testing cells are placed in the sun for a long period of time prior to use, temperature difference between the cell and the soil is not sufficient to cause alteration to the flow rate of soil gas from the soil into the cell.

Figure 3-6 indicates that a temperature difference of 50°K results in a pressure difference of approximately 3 pascal. Within temperature differences around 10 to 15 degrees, the

resulting pressure differences are less than 1 pascal.

Experimental observations of temperature and differential pressure in the testing assembly indicate differences that are of minimal concern regarding all soil samples tested. Figure 3-7 illustrates a two-and-a half-day time-dependent response of the test chamber temperature measured during the testing of a soil sample collected at depth of 3 feet. The temperature response followed very closely the temperature of the room where the assembly is located. The assembly was placed at the Concert Lab of the Department of Civil Engineering. This area is mainly open to the outdoors, and temperature in the lab is not controlled or conditioned.

Figures 3-8 and 3-9 show the corresponding time-dependent relative humidity in the test chamber and differential pressure between the test chamber and the surrounding air simultaneously measured with the temperature measurement in Figure 3-7. Monitoring of temperature temporal variations along with relative humidity in the test chamber and the corresponding pressure differentials across the chamber all indicated a range of values that are not substantial to cause invalidation of the soil-gas radon testing practice with respect to the temperature condition.

Figures 3-10, 3-11, and 3-12 and 3-13, 3-14, and 3-15 are provided to show samples of the above responses. The first set of figures (3-10 to 3-12) shows the time-dependent responses of temperature, relative humidity, and pressure

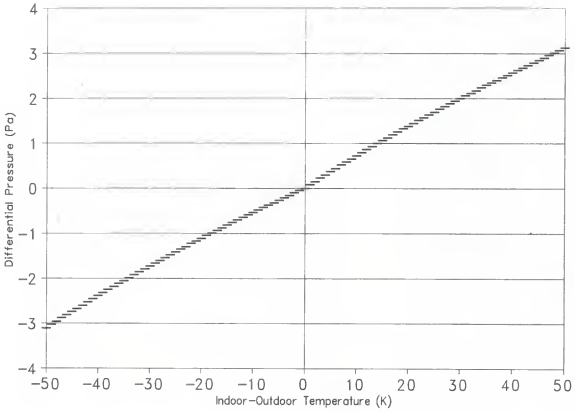

Figure 3-6: Predictions of the pressure differentials induced by temperature differences between two zones

differentials simultaneously collected during a two-and-a-half-day testing of water-saturated soil samples collected from a site in Gainesville (S3) at a depth of 4 feet. The second set of figures (3-13 to 3-15) also shows the time-dependent responses of temperature, relative humidity, and pressure differentials simultaneously collected during a two-and-a-half-day testing of original soil samples collected at the same site (S3) but from a depth of 2 feet.

Giving the range of temperature differences between outdoors and the soil, the limited effect of temperature-induced pressure differentials for temperature differences encountered between the testing cell and the soil, temperature does not adversely affect soil-gas testing prior to temperature condition should be satisfied if the testing cells are kept at relatively the normal air temperature.

Evaluation of the Soil Compaction Condition

The mechanical compaction of soil and fill materials (if used) at the construction site is a practice that is used to improve soil conditions for construction purposes.. In soils,the pore space is typically filled with gas (air) and liquid (water). The rest of the volume, other than the collective pore space, is filled with solid soil components. Although soil-gas and water content in the soil system are constantly changing, the practice of soil compaction during

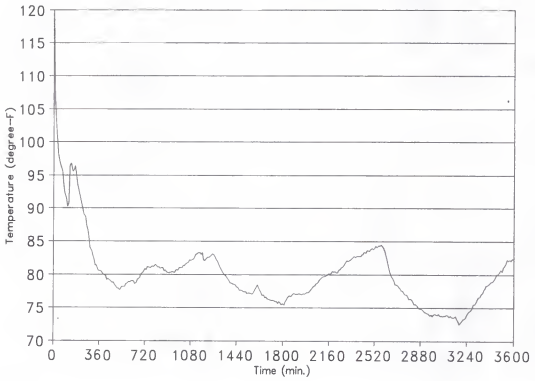

Figure 3-7: A two-and-a-half-day temporal response of the temperature inside the testing chamber for the dried configuration sample of site S1 collected at a 3-foot depth

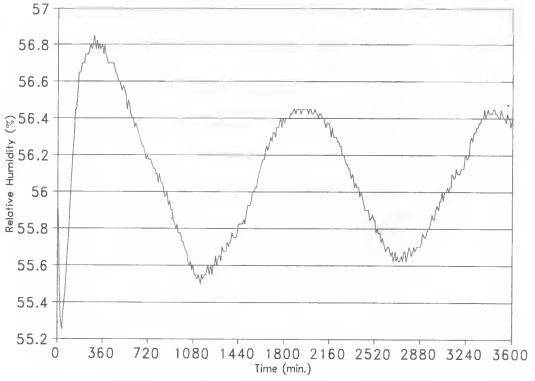

Figure 3-8: A two-and-a-half-day temporal response of relative humidity measured inside the testing chamber during the testing of the dried configuration sample of site S1 collected at a 3-foot depth

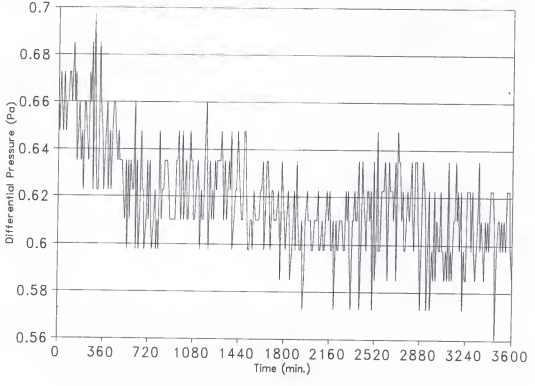

Figure 3-9: A two-and-a-half-day temporal response of the differential pressure between the testing chamber and the surrounding during the testing of the dried configuration sample of site S1 collected at a 3-foot depth

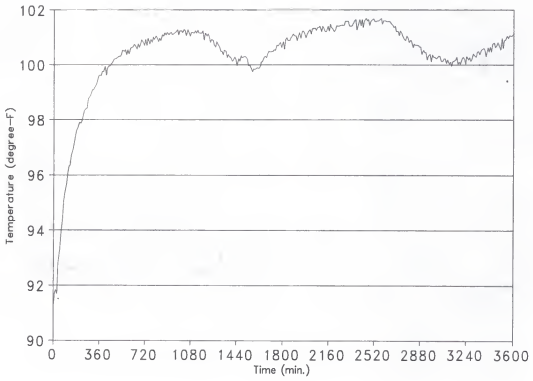

Figure 3-10: A two-and-a-half-day sample of the time-dependent temperature response in the testing chamber for the saturated soil sample collected from site 2 at a 4-foot depth

site preparation for construction forms a condition that is expected to adversely affected soil-gas testing if it occurs after the compaction. Soil compaction changes the pore space physical characteristics, resulting in increasing fluid flow resistance, and thus it might affect sampling of soil-gas radon drawn from the soil into the testing cell.

An applied load which reduces the total volume of soil causes compaction. Because the soil particles and water are relatively incompressible, compaction causes reorientation of soil particles and reduces the volume of air. This slows down water and air movement and reduces the water holding capacity of the soil.

Not only might the increase of air-flow resistance in the soil system affect the soil-gas testing, but also a reduction of the soil's water-holding capacity can indirectly affect soil-gas testing. This may alter radon emanation and the percentage of radon atoms that terminate their range in the soil pore where they become migrable. In addition to the effect on soil-gas testing, excessive soil compaction may result in poor drainage, increased energy for tillage, and reduced crop yields because of reduced water and air movement in the soil. It may also result in reduced rate of root growth, and delays in tillage, planting, and harvesting.

Ponding of water on the soil surface in wheel-track depressions and on turn rows that receive extra machine traffic usually show the first evidence of excessive

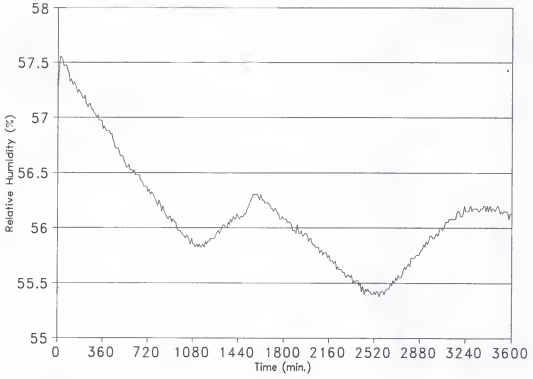

Figure 3-11: A two-and-a-half-day sample of the time-dependent relative humidity response in the testing chamber for the saturated soil sample collected from site 2 at a 4-foot depth

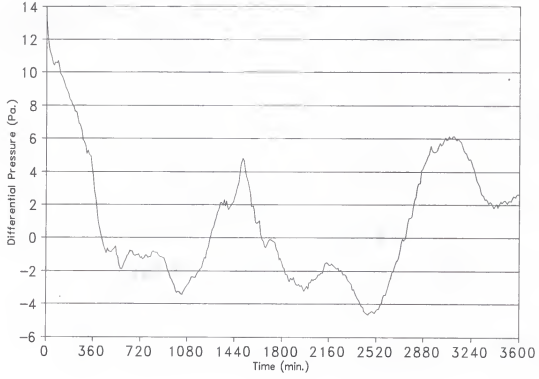

Figure 3-12: A two-and-a-half-day sample of the time-dependent differential pressure response across the testing chamber for the saturated soil sample collected from site 2 at a 4-foot depth

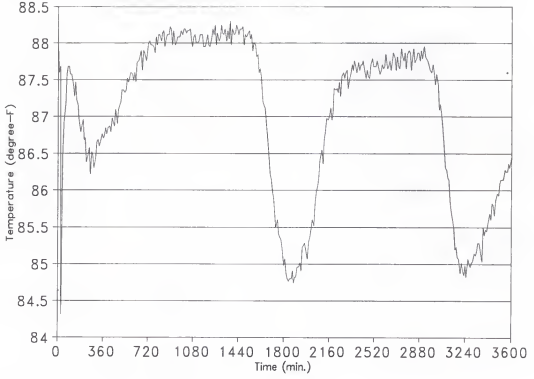

Figure 3-13: A two-and-a-half-day sample of the time-dependent temperature response in the testing chamber during the placement of the original soil sample collected at site 2 at a 2-foot depth

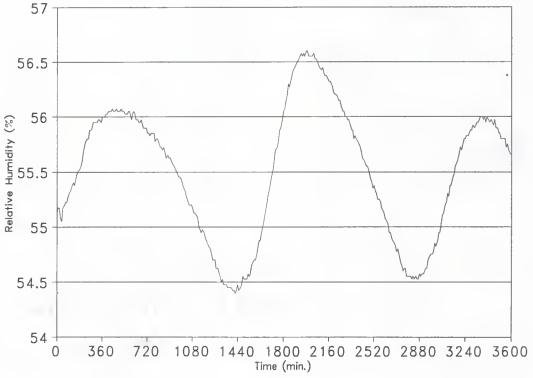

Figure 3-14: A two-and-a-half-day sample of the time-dependent relative humidity response in the testing chamber during the placement of the original soil sample collected at site 2 at a 2-foot depth

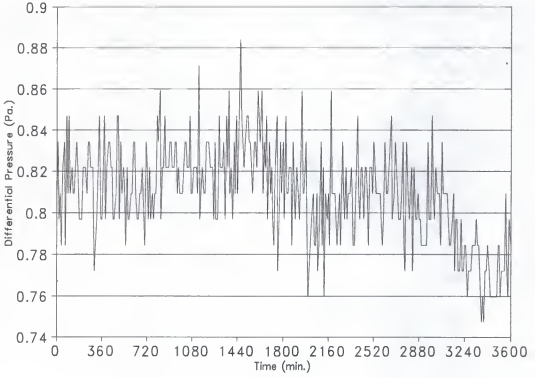

Figure 3-15: A two-and-a-half-day sample of the time-dependent differential pressure response across the testing chamber during the placement of the original soil sample collected at site 2 at a 2-foot depth

compaction. For the purpose of this research, detailed relationships between air permeability and soil compaction were not constructed based on theoretical or experimental approaches.

From a construction management standpoint, it is more suitable to recommend soil-gas testing prior to compaction as a preliminary part of a package in assessing the site. This allows avoiding many (or some) complications that could result from justifying testing results under compaction conditions.

Further, soils are complex systems and their compaction may be different from one site to another using the same load. Testing of soil-gas radon concentration is addressed here as a part of developing a construction-management approach. The results of testing can be used to initiate a decision about incorporating a radon-control system prior to construction.

Further, a decision to install a radon-control system should be made before soil compaction takes place, in most cases. Installing radon-control systems prior to construction should be implemented and conducted at an early preparation stage prior to soil compaction.

Therefore, in addition to avoiding potential misrepresentation of soil-gas testing results, testing results are needed before soil compaction if it is going to be used. Thus, for this application, the soil compaction condition can be minimized by requiring testing of soil-gas radon before soil compaction (if selected) as a construction-management

approach. The effect of soil compaction may be qualitatively assessed in a future research whereas findings may be readily incorporated into the findings of this research.

Observations and Evaluation of the Soil Moisture Condition

For most soils, only 10-50% of the radon generated actually emanates from the mineral grain and enters the pore volume of the soil (USDOI 1992). Depending on the relative position of formation and the direction of the recoil, the newly formed radon atom travels from its generation site in the solid grain until it loses its energy to the host materials.

The host materials could be the solid grain of the formation, another solid grain, or materials confined in the soil pore, primarily water and air. The transport range in water is approximately 600 times less than the range in air. This fact suggests that the soil water content may have a noticeable effect on radon availability in the pore space.

In fact, among the factors that influence radon emanation, soil moisture content has been demonstrated to have a significant impact (Strong and Levins 1982). Fluid-filled soil pores contain most of the soil moisture. When the content of water in the pore space increases, the direct emanation coefficient component is increased, since a greater fraction of the recoil radon atoms are trapped in the pore.

Soil moisture content consists of three components: gyroscopic, capillary, and gravitational. Most of the soil moisture effect is developed by the capillary component. This component is responsible for generating water films around solid grains that act as a trap for recoiled radon atoms.

The existence of water in excess of the capillary water will have a small effect on the radon emanation since most of the atoms are being stopped by the capillary water films. The gyroscopic component has only a minimal effect on emanation since it represents a very small percentage of soil moisture.

Although soil moisture content is expected to significantly affect the radon emanation coefficient, the focus of this section is to investigate whether soil moisture would interface with the testing of soil-gas radon concentration to a level that adversely affects the testing results.

Within the context of a construction management, testing of radon in the soil pore (soil gas) prior to construction has been evolving as an important measure by which the potential for elevated indoor radon concentration, after construction, may be predicted.

The above-mentioned measure may be used as the basis for managerial decisions on the need for applying radon-resistant construction standards. Furthermore, a continuing increase in such testing can be observed in the requirements for initial environmental assessment of sites prior to construction for

different purposes.

The block diagram of the experimental assembly used in this research to test the soil moisture effect on the testing of soil-gas radon concentration is given in Chapter 2 (Figure 2-2). Soil samples were placed on a wide, open-face pan with a soil thickness of approximately 5 cm.

The above design is utilized to minimize the effect of soil permeability and spatial dependency of the radon diffusion coefficient on the transport of radon from the soil sample into the chamber space. The chamber space was flushed with air prior to the start of each experiment.

Radon concentrations were then continuously monitored to observe the buildup of radon gas in the chamber until reaching equilibrium inside the chamber. Radon concentration, pressure, temperature, and relative humidity data were simultaneously measured with a sampling time of 10 minutes. Utilizing the data-logging system, data were retrieved from the logging system and automatically entered into a personal computer system.

Soil samples were collected from three construction sites, representing typical construction soils in Florida from three depths (2, 3, and 4 feet). These depths typically represent the usual range where in-situ soil-gas radon measurements are performed. The procedure used to handle soil samples is specifically designed to collect enough soil, which is divided into samples from the three depths. Collection of

soil samples from the three sites were avoided under abnormal weather conditions in the Gainesville area, such as heavy rain

Table 3-5: Soil samples identification system and corresponding sample configuration (O = original in situ, D = dried soil sample, S = water-saturated soil sample)

Site I.D.	Sample Identification	Collection Depth (ft.)	Code	Sample Configuration
S1	S1-1	2	O	Original
			D	Dried Soil
			S	Saturated Soil
	S1-2	3	O	Original
			D	Dried Soil
			S	Saturated Soil
	S1-3	4	O	Original
			D	Dried Soil
			S	Saturated Soil
S2	S2-1	2	O	Original
			D	Dried Soil
			S	Saturated Soil
	S2-2	3	O	Original
			D	Dried Soil
			S	Saturated Soil
	S2-3	4	O	Original
			D	Dried Soil
			S	Saturated Soil
S3	S3-1	2	O	Original
			D	Dried Soil
			S	Saturated Soil
	S3-2	3	O	Original
			D	Dried Soil
			S	Saturated Soil
	S3-3	4	O	Original
			D	Dried Soil
			S	Saturated Soil

and thunderstorms in an attempt to obtain samples that were as normal as possible. All samples from the three sites were

collected on sunny days and within a two-week period in September.

Samples were collected by excavating the soil, checking the depth, and retrieving the samples. Upon collection, samples were placed in airtight containers (site containers), sealed, labeled, transported, and stored in the concrete laboratory at the Department of Civil Engineering. Table 3-5 listed soil sample classifications and other sample characteristics used in these experiments.

Processing of soil sample site containers was performed at the department's soil laboratory. The contents of the site container were divided into three parts, where each part was placed in a smaller airtight plastic container (lab container).

A fourth sample was prepared for each site and each depth and used for measuring soil water content. The latter was performed by weighing the sample, placing the sample in a conventional oven for a minimum of two days, and weighing the sample at the conclusion of the heating. Table 3-6 shows the weights of soil samples and the corresponding soil moisture percentages obtained from measuring soil moisture at the soil laboratory of the Department of Civil Engineering.

Preparation of dry soil samples was performed using the same convectional hot-air oven for a minimum period of 48 hours. Dried samples were then placed in the lab containers,

Table 3-6: Results of soil water weights and sample water contents for the original and processes soil samples collected at the three construction sites at three depths

Soil sample I.D.	Sample weight (g)	Processed sample weight (g)	Sample container weight (g)	Sample water weight (g)	Soil water content (%)
S1-1O	176.8	167.4	33.5	9.45	9.6
S1-1D	176.8	173.5	33.5	0.94	0.67
S1-1S	238.2	201.5	19.5	36.68	17.9
S1-2O	94.8	89.8	33.3	0.94	6.7
S1-2D	154.9	153.7	33.4	1.21	0.99
S1-2S	229.6	195.2	35.4	34.44	17.6
S1-3O	168.2	159.4	33.4	8.77	6.6
S1-3D	167.4	196.7	33.4	0.33	0.2
S1-3S	234.7	191.8	33.4	35.73	17.8
S2-1O	195.3	178.4	33.4	16.85	10.4
S2-1D	168.2	182.9	33.4	1.21	0.8
S2-1S	253.8	210.1	33.4	43.7	19.8
S2-2O	225.7	207.2	33.4	18.51	9.6
S2-2O	210.1	208.9	33.4	1.21	0.7
S2-2S	258.2	212.0	33.4	46.15	20.5
S2-3O	214.5	191.8	33.2	22.69	12.5
S2-3D	191.8	191.7	33.2	0.13	0.8
S2-3S	281.4	241.5	33.2	39.91	16.0
S3-1O	154.9	123.7	33.2	31.19	25.6
S3-1D	162.6	161.6	33.2	1.07	0.8
S3-1S	208.1	151.3	33.2	56.77	32.4
S3-2O	151.5	123.4	33.2	28.10	23.8
S3-2D	133.1	132.9	33.2	0.18	0.2
S3-2S	236.9	166.5	33.2	70.39	34.6

Table 3-6 Continued

Soil sample I.D.	Sample weight (g)	Processed sample weight (g)	Sample container weight (g)	Sample water weight (g)	Soil water content (%)
S3-3O	197.7	167.8	33.2	30.49	18.5
S3-3D	167.2	166.8	33.2	0.33	0.2
S3-3S	226.6	172.4	33.2	54.21	28.0

sealed, labeled, and left for a minimum of 14 days prior to testing, allowing for radon to reach equilibrium with its parent. Saturated samples were prepared by adding water into soil samples until saturation. As with the prepared dried soil samples, saturated samples were placed in the lab containers, sealed, labeled, and left for a minimum of 14 days prior to testing.

Figure 3-16 shows the distribution of soil water contents for the in-situ (original) samples collected at the three construction sites in Gainesville. Although no control is available on the in-situ soil moisture, observation of soil moisture in the original samples shows a gradual increase in amount of water hold in the soil pore space. The soil moisture of the samples collected at the first construction site (S1) shows little change as sampling goes from soil surface to 4 feet deep, and all were below 8% by weight of water content.

Samples collected from the second construction site (S2) show a water content profile that is slightly decreased as the

depth increases. Soil water moisture started at approximately 10% by weight at the first 2 feet, dropped to 9% at another feet, and increased to more than 12% at a depth of 4 feet.

Soil moisture profiles for the in-situ samples collected at the third construction site were systematically lower as the sampling depth increases. Soil moisture dropped from approximately 25% at a sampling depth of 2 feet to 18.5% at a sample depth of 4 feet. The overall distribution of in-situ soil moisture as shown in Figure 3-16 provides for an overall range of soil moisture content expected to cover most soils suitable for normal construction.

Figure 3-17 shows soil moisture distribution for the processed (dried) soil samples collected from the three depths at the three construction sites. Processing of these samples started from the same in-situ soil collected from the site. Drying in the context of these experiments consisted of environmental drying to simulate dry soil conditions as naturally as possible.

In-situ samples were first drained of gravitational water, under the effect of gravity, and then left open while being exposed to sunlight in a covered area for a minimum of 12 hours before measurement. Soil samples were then weighed and placed in a conventional oven where they remained for a minimum of 48 hours. Finally, samples were weighed again to calculate soil moisture.

The calculated soil moisture represents the dry soil

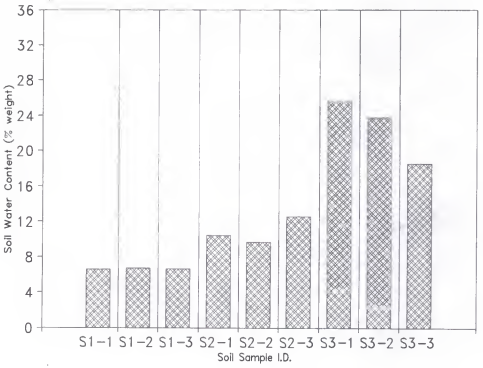

Figure 3-16: Distribution of soil water content of the original soil samples collected at the three construction sites for depths of 2, 3, and 4 feet, respectively

condition, as is expected to be present at the construction site when soil-gas testing is conducted. Differences in soil moisture, as seen in Figure 3-17, ranged from 0.1% to 1% by water weight. The small differences among the samples are attributed to specific soil characteristics, such as the ability to hold a very small quantity of water, even after being subjected to 48 hours of drying.

Figure 3-18 shows the distribution of soil water content for the processed saturated soil samples from the three construction sites and the corresponding sampling depths. Processing of soil samples under the saturation conditions attempted to simulate saturated soils that might exist due to rain or other environmental conditions while soil-gas radon testing is conducted or is to be conducted. Saturation conditions were introduced by partially flooding the in-situ (original) soil samples with water and placing them outdoors for a minimum of 12 hours. Samples were then weighed, dried in the convectional oven for a minimum of 48 hours, weighed again, and their moisture contents calculated.

The resulting saturated soil samples that were placed in the testing chamber of Figure 2-2 had a moisture content range from slightly more than 15% to slightly lower than 35%. Samples collected from construction site S3 show the maximum holding of water in their pore spaces, which is consistent with the processed samples under dry soil conditions.

Figure 3-19 provides a plot to compare the distribution

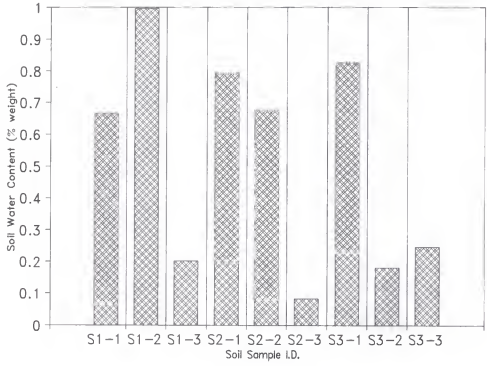

Figure 3-17: Distribution of soil water content of the processed dried soil samples collected at the three construction sites for depths of two, three, and four feet, respectively.

of soil water content (% weight) for the original in-situ and processed dry and saturated condition soil samples collected from the three construction sites at depths ranging from 2 to 4 feet below grade. The average soil moisture content level from in-situ samples (original soils) was generally higher for samples collected at the corresponding sites S1, S2, and S3, respectively. In the original samples, maximum and minimum soil water contents were 25.64% and 6.60% weight, both collected at the 2-foot depth in S3 and S1, respectively.

Figure 3-20 shows the overall maximum range of soil moisture variation observed in all the samples including the dry and saturation conditions. The maximum change in soil moisture, due to processing, occurred in the 2-foot depth sample collected from the construction site S1. Soil water content was altered by more than 11% of weight due to the processing. The minimum change occurred in the 4-foot sample collected from construction site S2 with a range of less than 4% of weight.

The majority of soil samples exhibited an alteration of soil moisture content by at least 9% of weight when they were processed through the saturation condition compared to the dry conditions.

The maximum consistency of soil moisture alteration response was observed in the samples collected from construction site S1, while the most volatile response was exhibited by the samples collected from construction site S2.

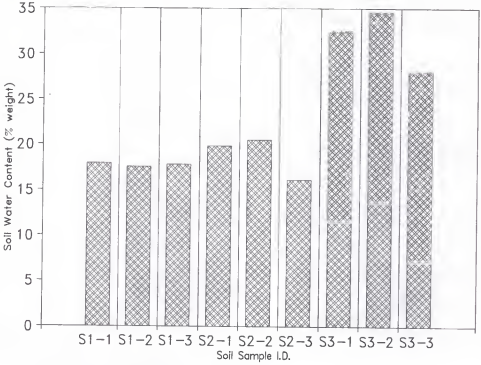

Figure 3-18: Distribution of soil water content of the processed saturated soil samples collected at the three construction sites for depths of two, three, and four feet, respectively.

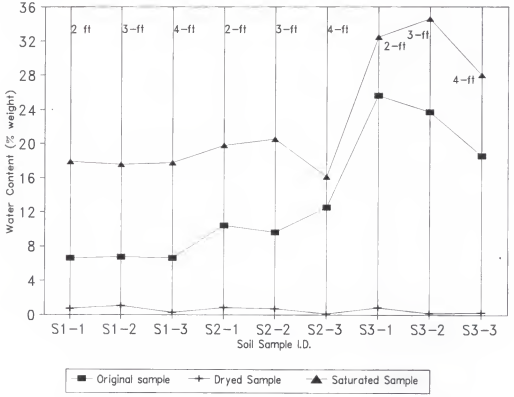

Figure 3-19: Illustration of the original, dried, and saturated soil samples water contents collected from two to four feet below grade from the three construction sites in Gainesville.

Radon concentrations were monitored in the test chamber for the original and the processed soil samples as they may exist naturally at the site during soil-gas radon testing prior to construction. Figure 3-21 shows the measured average radon concentrations in the test chamber generated from the original soil samples collected from the three construction the original soil samples collected from the three construction sites at sampling depths of 2 to 4 feet.

In-situ soil samples from construction sites S1 and S2 developed radon concentrations in the testing chambers that averaged between 10 to 11 pCi/l at the three sampling depths. Soil obtained from construction site S3 developed higher average radon concentrations by approximately 30% than the other construction sites at the three sampling depths. This is attributed to higher concentrations of radium in the soil at construction site S3. The maximum average radon concentration obtained from the in-situ (original) condition developed in the 2-foot sample from construction site S3 at approximately 14 pCi/l.

Figure 3-22 shows the distribution of average radon concentration of the three construction sites at the three depth samples for the dry preparation condition. The overall concentrations measured in the testing chamber are lower than the in-situ samples by a minimal margin. The profile of the average radon concentrations for the dry soil condition was similar to that associated with the in-situ condition. The

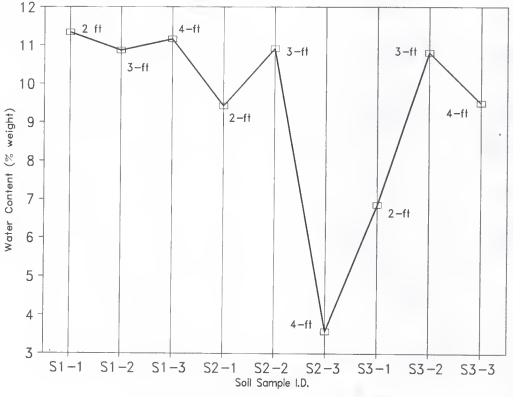

Figure 3-20: The maximum range of soil moisture variation observed among original and processed samples collected from 2 to 4 feet below grade from the three construction sites in Gainesville

maximum average radon concentration was also developed from the 2-foot sample of the construction site S3 with a level of approximately 12.5 pCi/l.

Figure 3-23 shows the distribution of the average radon concentration measured in the test chamber for the saturated soil samples. The observed concentrations are comparable with those from the in-situ and the dry soil conditions, except for the 2-foot sample collected from construction site S1, which showed a drop in the emanated radon by approximately 50% and was inconsistent with the rest of the test results.

Although the overall profile in Figure 3-23 looks different than those illustrated in Figures 3-22 and 3-21, the profiles (except for the inconsistency above) are similar and comparable. The shape of the plot in Figure 3-23 is influenced by the 50% reduction in the average radon concentration that occurred at the 2-foot sample collected at construction site S1.

Figure 3-24 shows the maximum range of average radon concentration variations that resulted due to drying or saturating the in-situ samples and in relation to the in-situ soil samples. Except for the 2-foot sample above (S1-1), the maximum alteration in average radon concentration measured in the testing chamber due to the range of soil water moisture from dry to saturated was approximately 2 pCi/l among all samples combined.

Figure 3-25 illustrates the comparative responses of

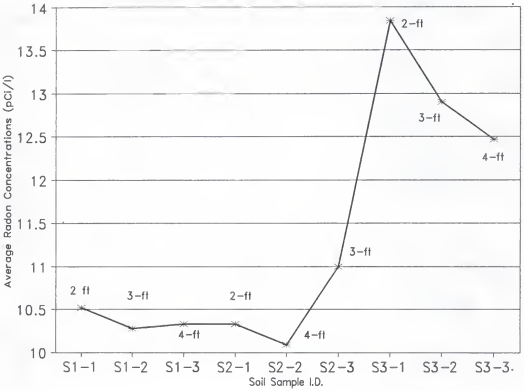

Figure 3-21: An illustration of the average radon concentrations measured at the testing chamber for the original soil samples collected from the three construction sites at two to four feet depth.

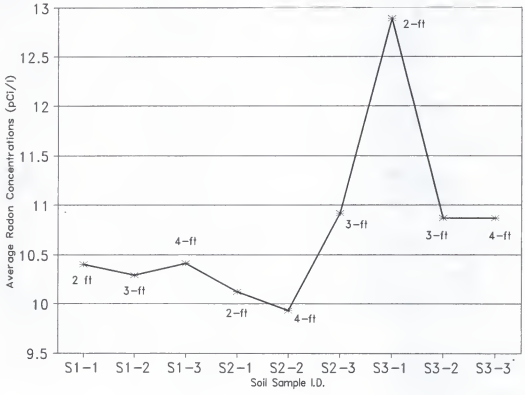

Figure 3-22: An illustration of the average radon concentrations measured at the testing chamber for the dried soil samples collected from the three construction sites at depths of 2 to 4 feet

average radon concentration plotted for original, dried, and saturated soil samples collected at the construction sites from 2- to 4-foot depths. As seen in the graph, minimal deviation of average radon concentrations was observed between the dried to saturated soil samples and the original soil sample, particularly for sites S1 and S2. Samples collected from site S3 experienced some differences between the dried/saturated samples and the original; however, these differences were small.

The differences between the maximum and the minimum time-averaged radon concentrations (concentration span) measured at the assembly chamber for all samples were comparable except for the 2-foot depth at site S1. This sample showed a concentration span value that significantly differs from the rest of the samples; therefore, it is omitted from consideration.

The span of time-averaged radon concentration is calculated as

$$Rn_{span} = ABS[Rn_{saturated} - Rn_{dried}]$$

where ABS refers to the absolute value of the difference. Rn_{span} (pCi/l) represents the range of average radon concentration changes corresponding to the range of soil water content from dryness to saturation.

Ignoring the soil sample collected at a 2-foot depth in site S1, the maximum span of the average radon concentration among soil samples was observed at a depth of 4 feet in site

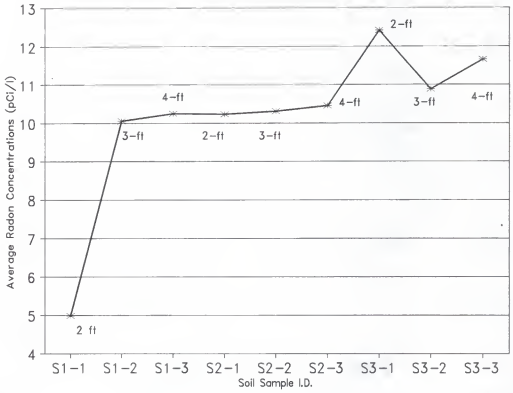

Figure 3-23: An illustration of the average radon concentrations measured at the testing chamber for the saturated soil samples collected from the three construction sites at two to four feet depth.

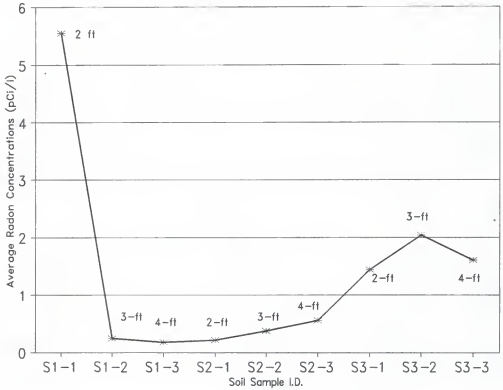

Figure 3-24: The maximum range of average radon concentration variations measured at the testing chamber for all soil samples collected from the three construction sites in Gainesville

S3, and it is approximately 1 pCi/l. Such a span is very small and is expected to have a minimal effect on the predicted average in-situ soil-gas radon concentration (Slimitari et al. 1996).

It should be noted that since the same experimental setup used for collecting the radon emanated from the soil samples, it can be safely assume that errors that may be introduced due to instrumentation are the same. Further, the standard deviation, or the variance, in the measured quantities of radon is mainly the square root of measured quantity in each reported value. This variance is due to the radioactive decay process, which can be reasonably represented by Possion distribution. However, since only the qualitative behavior of the average radon concentration, measured in the testing assembly, with respect to the soil water content is of concern, it can be safely assumed that similar and comparable uncertainty is exhibited in the average radon concentrations reported for the samples.

Accordingly, for the purpose of this research, the relative change in the average radon concentration emanated from the soil sample under conditions of saturation and dryness may be used as a qualitative indicator to the relationship between the average radon concentration and the soil water content. Furthermore, detailed analysis of the uncertainty in the measured radon concentrations and then in the calculated average radon concentrations will not change

the qualitative behavior of the average radon concentration with respect to the soil water content since comparable uncertainties, with minimal differences, are incorporated into all the points of the qualitative comparison.

To represent the span of radon concentrations measured with original soil samples without alteration to their water content, the following parameter may be utilized:

$$Rn_{ratio} = 100 \times (Rn_{span}/Rn_{original}) = 100 \times (ABS[Rn_{saturated} - Rn_{dried}]/Rn_{original})$$

where Rn_{ratio} (%) represents the ratio of time-averaged radon concentration span to the time-averaged radon concentration measured with original soil. This parameter indicates the percent change of averaged radon concentrations measured in the assembly chamber, with soil water content alteration from dryness to saturation, to the radon concentration measured from the original soil sample without water content alteration.

Figure 3-26 shows the percent change in measured radon concentrations with water content alteration with respect to original soils.A maximum change of approximately 6% was observed in the 4-foot sample collected at site S3. Soil water content alterations for samples collected at S1 and S2 were less than 3% and 5%, respectively, with respect to radon concentrations of original soil samples.

These changes in radon concentration due to alteration of soil water content are very small. The scope of such changes

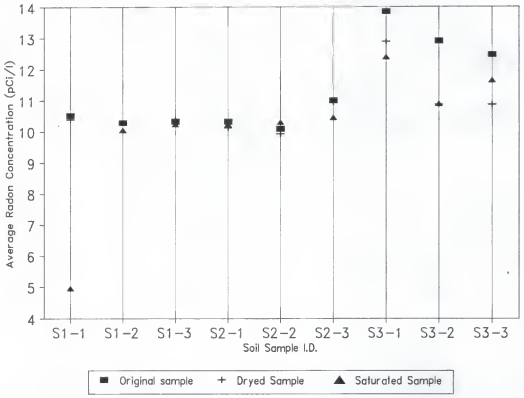

Figure 3-25: The time-integrated response radon concentrations for original, dried, and saturated soil samples measured in the testing chamber

indicates that only a minimal effect, on the order of less than 10%, may be experienced during in-situ soil gas radon measurement.

Although a large impact of soil moisture on radon emanation from the solid soil grain into the pore space has been demonstrated by several researchers in uranium tailing (Stranden et al. 1984, Strong and Levins 1983), soil moisture significance on gaseous radon concentration in the collective pore space at the macroscopic level is minimal.

On the microscope level, the effect of soil moisture is particularly significant when alteration to the soil moisture capillary component occurred. Trapping of recoiled radon atoms, generated from radioactive decay of radium in the pore space, is profoundly reduced when capillary water surrounding a solid grain is reduced or eliminated. Alteration to the soil water content in the gravitational water (toward saturation) is expected to have a minimal effect on the trapping of recoiled radon atoms transported from the soil solid grain into the pore space, since most atoms trapped in the capillary water film around the solid grain. In this scope, alterations of water content in tested samples during saturation were expected to have less effect than alterations toward dryness.

Except for the sample collected at 2 feet in site S1, where measured radon concentration dropped by more than 50% during dried-sample testing, samples tested during soil

dryness conditions show little alteration to radon measurement performed during original water moisture contents and saturation conditions.

Testing of radon concentration associated with samples designed to simulate in-situ soil under the possible range of soil water content (from dryness to saturation) indicated only a minimal effect of the latter regarding the gaseous radon availability in the pore space of soil. For the purpose of soil-gas radon testing as a procedure to be used for a construction-management approach toward incorporating a radon-control system prior to construction, the soil water content condition does not show sufficient evidence of the ability to alter soil-gas testing results. Therefore, the soil water moisture condition does not invalidate the representation of soil-gas radon testing within the soil conditions examined in this research.

The Construction-Management Approach

To justify incorporating the developed soil-gas radon testing procedures into a framework that the construction manager can implement, the advantages of such implementation should be briefly discussed. Testing of soil-gas radon concentration can provide a tool through which a quantitative measure of radon concentrations in the construction site may be assessed.

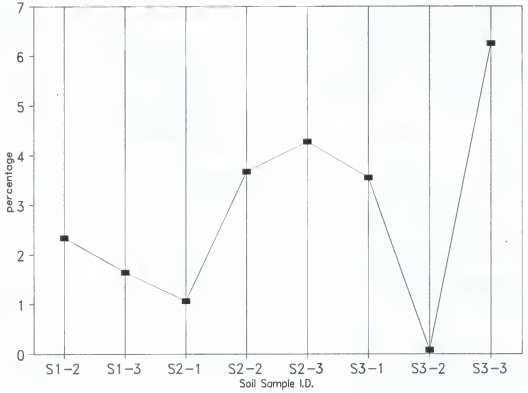

Figure 3-26: An illustration to the changes in the measured average radon concentration of original in-situ soil samples in response to the range of soil water moisture from dryness to saturation.

All related parties to the construction industry, such as designers, project engineers, construction managers, builders, and consultants, can utilize the assessment results obtained from soil-gas radon testing, prior to construction, to facilitate the decision of incorporating radon control systems into the building plans. The general areas in which advantages are realized can be divided into three main areas:

(1) cost savings associated with incorporating indoor radon preventive measure during construction compared to after the completion of the building;

(2) minimization of the general liability of involved parties concerning the issue of indoor radon problems; and

(3) significant improvement to the public health and sales and advertisement advantages resulting from providing buildings that are free from elevated indoor radon concentrations.

Incorporating radon preventive and control measures during the construction process provides significant advantages in the overall construction-management operation and the delivery of the contract. Construction plans that incorporate radon preventive measures, when needed, in the design phase and prior to the construction phase could substantially reduce the cost of this preventive measure when compared with the same measure taken after the building's completion.

Most radon preventive and control systems are installed

in the substructure area and extended through wall cavities. Thus when their installation takes place during construction, costs are minimized through savings in the labor associated with installation.

More importantly, when the substructure areas are accessible, during construction, designing indoor radon prevention and control systems is significantly easier and more efficient. The result is both lower capital and operating costs when compared with systems designed to meet the same need but installed after construction.

The second area of advantage is realized through minimizing the general liability that all related parties to the construction operation carry. Builders, designers, owner, and construction managers will continue to be liable if elevated indoor radon concentrations are found in the completed building.

Although regulatory laws related to such liability specifically addressing indoor radon are under development, general liability is established through other legal requirements of providing buildings that are safe and do not have an inherent item that would affect the resale value of the property. General liability in this issue can be and have been established in common law practices.

The third area of advantage is the improvement to the public health, advantages in the sale and advertisement operation, and the general image of the construction company,

consultant, construction manager, or owner.

Since indoor radon problem, by definition, does not exist except after the complete closing of the structure, which for legal purposes means after the issuing of the certificate of occupancy, there is no direct quantitative measure that could be applied to facilitate the managerial decision of incorporating radon prevention systems prior to construction. Soil-gas radon testing is the only available parameter to be measured, prior to construction, which can be used to provide a direct indicator of the potential of a future indoor radon problem after the completion of the structure.

There has been a remarkable increase in the testing of radon concentration in the soil prior to construction which has been generally approached to provide a preliminary evaluation of construction sites. This evaluation is being employed by engineering and construction companies, contractors, consultants, engineers, architects, and owners in an attempt to minimize their general liability.

Testing of soil-gas radon concentration is being specifically noticed as an emerging practice of packaging soil-gas radon testing as a part of the first- and second-phase environmental assessments of the construction site.

Despite the emerging practice of soil-gas radon testing and the potential advantages of developing this practice into a construction-management approach, there are neither standard testing procedures nor management approaches in employing and

managing such approaches.

As a result of not having an appropriate framework and procedure upon which testing of soil-gas radon concentration and the utilization of testing results may be effectively pursued, the practice of employing soil-gas radon concentration testing results is not yet appropriately developed. Many testing results may not be representative since testing conditions are not considered. This contributes to much lower efficiency in the associated management decisions and process.

An appropriate framework addressing the development of soil-gas radon testing procedures, and therefore the formation process of a construction-management approach, can be achieved by incorporating the experimental and theoretical results discussed in this chapter.

The construction-management approach must incorporate all the results previously addressed with the applicable, but flexible, procedures that would allow adequate assurance against adverse conditions. Considering the advantages briefly discussed above, soil-gas radon testing prior to construction must be included in any construction management operation involving residential or large structures that people will occupy.

Based on the experimental setup used in this research, and within the limitations of the specific procedures discussed throughout the text, Table 3-7 briefly summarizes

the type of the investigation approach used in this research to assess the effect of the experimental setup configuration (as used in this research), the temperature condition, and the soil water content. Further, Table 3-7 shows the potential effect of the testing configuration condition, the tempertaure condition, and the soil water content on the resulted soil-gas average concentration when measured at the site using the experimental setup discussed in this research. The corresponding expected contribution for each of the above three conditions to potentially alter the results of the soil-gas radon testing, using the experimental setup of this research, when performed in-situ prior to construction is also given in Table 3-7.

Table 3-8 shows the recommendations as to the degree of necessity to incorporate a precaution, or the procedure as developed in this research, into the practice of testing soil-gas radon prior to construction for the experimental setup configuration condition, the tempertaure condition, the soil compaction condition, and the soil moisture condition. Accordingly, table 3-8 briefly summarizes the directions that the construction management operation (or the construction manager) should follow in designing, developing, and executing soil-gas radon testing at the construction site, as well as in addressing the need for soil-gas radon testing prior to construction, and consequently the incorporation of radon control systems.

Table 3-7: A brief summary of the investigation approach, potential effect, and potential contribution to soil-gas radon testing result misrepresentation for testing (setup) configuration condition (A), temperature condition (B); soil compaction condition (C), and soil water content condition (D).

Testing Code	A	B	C	D
Item				
Investigation Approach	experiment-al	theore-tical	manag-erial	experime-ntal
Potential Effect	significant	minimal	not asses-sed	minimal
Contribution to Result Miss-representation	substantial	very limited	not asses-sed	minimal

Table 3-8: A brief summary of the recommendation for the degree of necessity to incorporate precaution or procedures developed in this research in designing, developing, and executing soil-gas radon testing to support the construction management decision for incorporating radon control system(s) installation prior to construction. Testing codes are: A = testing (setup) configuration condition, B = temperature condition, C = soil compaction condition, and D = soil water content condition.

Testing Code	A	B	C	D
Incorporation Recommendation	must	recomm-ended	must	should

CHAPTER 4
SUMMARY AND CONCLUSIONS

It should be acknowledged that the testing apparatus used in this research, i.e Pylon AB-5 with 300A standard scintillation cell and 5/16 inner diameter tubing, is widely used for testing soil-gas radon concentration in the field (construction site). However, it is important to note that the findings of this research and therefore the presented recommendations are applicable within the configurations limited by the scope of the testing apparatus, procedures, and conditions used and identified earlier in this research. It is further acknowledged that several variations to the used configurations are possible and such variations may render one or more of the research's findings and the following recommendations invalid. Accordingly, the following recommendations must be viewed within the scope of the radon testing configurations, the testing apparatus, and the procedures used in this research.

Testing of soil-gas radon concentration can provide a tool by which a quantitative measure of radon concentrations in the construction site may be assessed. Managers, engineers, builders, and architects may utilize assessment

results obtained from soil-gas radon testing, prior to construction, to facilitate decisions on incorporating radon control systems into the building plans.

Soil-gas radon testing is one of the available parameter to be measured, prior to construction, which can provide a direct indicator of the potential for future indoor radon problems after the completion of the structure. Accordingly, increasing attention has been given to an emerging practice that packages soil-gas radon testing as a part of the first- and second-phase environmental assessments of the construction site.

Three conditions associated with the soil-gas radon testing, which might affect the testing prior to construction, have been addressed in this research. These conditions are: the condition of temperature difference between the testing system and the soil gas, the condition of the testing configuration that is used to test the soil gas, and the condition of soil moisture at the site during the time when the soil sample is collected. A fourth condition that is expected to affect soil-gas radon testing is the condition of soil compaction. Since the condition of soil compaction was not addressed by this research but is it may potentially affect the testing of soil-gas radon, it is recommended that soil-gas radon testing to be conducted prior to compacting soil at the construction site.

It should be noted that the above recommendation,

concerning the condition of soil compaction, is drawn from a managerial standpoint rather than from quantitative investigations. This recommendation is developed to avoid potential interferences between soil compaction and soil-gas radon testing giving the case in which the effect of the former on the latter is not assessed (or known). This recommendation may be altered, canceled, or modified when the effect of soil compaction on the testing of soil-gas radon is adequately addressed or become known. Accordingly, experimental, theoretical, and managerial approaches may be used to investigate the above conditions and to qualify the testing of soil-gas radon concentration within their contexts and effects.

The condition of temperature can be evaluated through both theoretical and experimental investigations. Adverse effects can be realized if temperature difference between the soil gas and the testing cell is large enough to create a pressure difference that can alter the flow of the soil gas from the soil into the cell (that is used to collect the soil gas).

There is an indirect relationship between the temperature of the soil-gas in the pore space of the soil and the testing call. This relationship is expected to have an indirect effect on the soil-radon gas concentration when measured, using the testing configuration described in this research,

prior to construction. The influence of temperature on the testing results mainly depends on the size of temperature difference between the testing cell and the soil gas. The range of temperature differences between the site's soil and the testing cell is generally very small. However, the temperature of the soil gas at depths of 2 to 4 feet, where soil gas is typically drawn for the purpose of the soil-gas radon testing, is not a parameter under the tester's control. Therefore, attention can be given to the temperature of the testing cell, which can be controlled by the tester, to minimize any temperature difference (of concern) between the soil gas and the testing cell.

The temperature-induced pressure differential model can be used to predict pressure differences induced over a range of temperature differences associated with soil-gas radon testing and thus to evaluate the temperature condition. Temperature difference is not expected to be large between the soil zone (or area) where the soil-gas radon testing tube is located and the testing cell. Experimental observations of temperature and differential pressure in the testing assembly indicate differences that are of minimal concern in all soil samples tested.

Given the range of temperature differences between outdoor and the soil and the limited effect of temperature-induced pressure differentials for temperature differences encountered between the testing cell and the soil,

temperatures do not adversely affect soil-gas testing prior to construction. From the viewpoint of testing conditions, the temperature condition should be satisfied if the testing cells are kept relatively close to the normal ambient temperature. Therefore, the temperature condition does not have an adverse effect on the soil-gas radon testing, and the construction manager or other interested parties need only to use common-sense precautions as far as the temperature condition is concerned.

The effects of the condition of soil compaction may be developed from the mechanical compaction of soil and fill materials, when exist, at the site for different purposes, mainly for soil preparation during construction. Soil compaction forms a condition which may alter soil-gas testing results if the testing occurs before and after the compaction. For example, soil compaction changes the pore-space physical characteristics. The change in the pore-space may result in increasing fluid-flow resistance and thus might affect the sampling of soil-gas radon that is drawn from the soil into the testing cell.

As discussed above, in this research and based on the managerial concept of avoiding the unknown, it is recommended that testing of soil-gas radon to be conducted prior to soil compaction, if soil compaction is to take place at the construction site. This recommendation not only provides for avoiding any possible interference between the soil compaction

and the radon testing performance, but also provides for potential savings in simplifying other managerial aspects that may be related to both the soil compaction and the testing of soil-gas radon, such as scheduling and liability.

Based on the experimental radon testing setup used in this research , it has been shown that the effect of the testing configuration condition is mainly related to the length of tubes (or collection lines) that are used to collect the soil gas in the process of testing. Further, tube or line length is generally the item of the soil-gas radon testing configuration that enables maximum variation depending on the user or the tester. It should be noted that at the field, the length of the tube is the most likely element to be altered during the testing. Further, attention should be given to the diameter of the tube. Testing configurations that use tubes with different diameters than the one used in this research may exhibit different effects. However, the general scope of observations points out to the importance of insuring appropriate sizing and compatibility in the testing configuration, including the tubing and the suction pump.

The experimental investigations conducted in this research have shown that alteration of the soil-gas tube length can directly influence pressure differentials and flow rates associated with the testing configuration. Average radon concentrations reported in soil-gas testing decrease with the increase in the soil-gas tube length. Therefore,

appropriate tube length is significant in terms of validating the condition of the experimental setup to test for soil-gas concentration as a potential indicator of the need to incorporate a passive or active radon control system prior to construction. The tube configuration, including length as well as diameter, to be used in the testing procedure must be selected within limits that does not interfere with the pumping capacity of the experimental setup.

If the soil-gas collection time is not sufficient, the content of the system scintillation cell volume is not representative of the soil gas; it is at lower radon content, resulting in lower radon concentration when samples are measured after the 4-hour waiting period. The procedure to test for soil-gas radon concentration prior to construction as a potential to indoor radon problems must consider the compatibility of the radon collection tube and the sample collection time, as well.

Based on the above observations, Alpha counts should be be monitored during the collection of soil gas during the radon testing. The tester may then establish a plateau from the sniff counting results before collecting the grab sample. The latter ensures that a representative sample is obtained and thus minimizes adverse effects of the testing configuration conditions on soil-gas radon testing.

Experimental results showed very small changes in radon concentration obtained from soil-gas radon testing setups due

to alteration of soil water content. The scope of such changes indicates that only a minimal effect, on the order of less than 10%, may be experienced during in-situ soil-gas radon measurement due to fluctuations in natural soil water content.

Alteration to the soil water content in the gravitational water (toward saturation) is expected to have a minimal effect on the trapping of recoiled radon atoms transported from the soil solid grain into the pore space, since capillary water film, around the solid grain, is sufficient to trap the majority of the radon atoms that are emanated from the solid grain into the pore space. In this scope, alterations of water content in tested samples during saturation were expected to have less effect than alterations toward dryness. It should be noted that dryness and saturation conditions for the tested soils were developed for the purpose of qualitative assessment. The exact percentage of water content is not the concern of this research. However, the experimental procedure used in this research ensures that a reasonable range of soil water content (from dryness to saturation), or soil water content fluctuations were induced (around the natural soil water level) in the samples tested. This range (or fluctuations) is generally wider than the typical fluctuations at the site when the construction occurs, or to be occurred. It should be noted that in the majority of the cases, construction (specifically pouring of the building slab) does

not take place if environmental conditions at the site is severally abnormal. Accordingly, the induced soil water content range covers the potential scope of soil water content variations that may exist at the site when soil-gas radon testing is performed.

Based on the above, for soil-gas radon testing to be used as a basis for a construction-management approach to incorporating a radon-control system prior to construction, the soil water content condition does not show sufficient evidence of influencing later soil-gas testing results. Therefore, the soil water moisture condition does not invalidate the representation of soil-gas radon testing.

The construction-management approach to soil-gas radon testing should accommodate for the conditions of soil-gas radon testing related to tube length and soil compaction. Under those conditions, incorporation of the testing practice must adopt a procedure to monitor alpha count during sniff sampling for the purpose of establishing a count plateau and in scheduling the testing before soil compaction if it is needed for the site.

The construction-management approach to accommodating the conditions of temperature and soil water content must adopt a practice to ensure appropriate storage and handling of the testing cells and schedule soil-gas radon testing under normal environmental and soil conditions.

This research mainly addresses the environmental, soil,

and testing system configuration conditions that might affect the outcome of the soil-gas radon testing results. Findings of this research are integrated into testing a procedural development for constructing and optimizing a practical approach for the construction-management function and operation. Further, findings of this research are applicable to the specific experimental setups used in the investigations. Different experimental setups may alter the findings. Accordingly, the current recommendations should be considered within the scope of the experimental setup used in the research. It is recommended that the soil-gas testing configuration, as described in this research, be used in testing soil-gas radon concentration at construction sites prior to construction.

Several areas addressed in this research may form the basis for conducting additional research to investigate the overall approach of construction management, relationships among the testing conditions, testing devices development, and policy development.

The following future works are recommended as an extension of the current research.

(1) Experimental investigations and theoretical modeling of the effect of soil compaction on the testing of soil-gas radon testing procedures are recommended. Experiments may be developed by constructing a suitable airtight assembly that provides controlled passages for air and the capability to

apply pressure on soil samples. Different loads, representing typical soil-compaction operations, can be applied to the soil samples while air flow is measured throughout the sample. Results may be used to construct mathematical modeling and/or be integrated into a theoretical framework. This may be developed from Darcy's law and other theories describing fluid flow in porous media. This research would permit the establishment of correction factors or alternative testing procedures that would allow for soil-gas testing after soil compaction.

(2) Development of an integrated measurement system is recommended for the specific purpose of testing soil-gas radon concentration prior to construction. There is no integrated system design for the practical purpose of testing soil-gas radon concentration prior to construction. Available testing assemblies were designed for different purposes, mainly using the scintillation cell approach. The proposed system must incorporate measures for the four conditions addressed in the current research and associated correction factors.

(3) It is recommended that the current research findings be incorporated into a systematic investigation for the purpose of developing national soil-gas radon testing standards. These must address varieties of soils and fill materials at the construction sites and environmental conditions in a matter suitable for integration into codes.

(4) A cost-benefit analysis is recommended for the

expenses associated with testing soil-gas radon concentration prior to construction, the cost of incorporating indoor radon preventive and control measures, construction-management details related to implementing indoor radon preventive and control measures during construction, savings realized for such applications, management advantages in sales and advertising, and benefits realized from minimizing or eliminating general liability.

(5) It is recommended that the current research findings be incorporated into an implementation analysis study to integrate soil-gas radon testing procedures and the associated construction-management approach into newly developed or in developing radon-resistant construction standards for residential and large building construction, nationally or on a state basis, such as in the state of Florida.

REFERENCES

Al-Ahmady, K. K. 1995. Measurements and theoretical modeling of radon driving forces and indoor radon concentration and the development of radon prevention and mitigation technology. Ph.D. diss., University of Florida.

Al-Ahmady, K. K. 1992. Measurements and theoretical modeling of a naturally occurring ^{222}rn entry cycle for structures built over low permeability soils. Master's thesis, University of Florida.

Beer, T. 1976. *The aerospace environment*. New York: Springer-Verlag.

Bird, R. B., W. E. Stewart, and E. N. Lightfoot. 1960. *Transport phenomena*. New York: John Wiley and Sons.

Blair, T. A., and R. C. Fite. 1965. *Weather elements*. Englewood Cliffs, N.J.: Prentice Hall.

Brookins, D. G. 1990. *The indoor radon problem*. New York: Columbia University Press.

Browne, E., and R. B. Firestone. 1986. In *Table of Radioactive Isotopes*, edited by V. S. Shirley. New York: Wiley-Interscience.

Bossus, D. A. W. 1984. Emanating power and specific surface area. *Radiation Protection Dosimetry* 7:73.

Clements, W. E., and M. H. Wilkening. 1974. Atmospheric pressure effects on ^{222}rn transport across the earth-air interface. *Journal of Geophysical Research* 79, no. 33:5025-5029.

Cohen, B. L. 1990. Surveys of radon levels in homes by University of Pittsburgh radon project. Proceedings of the 1990 International Symposium on Radon and Radon Reduction Technology, Atlanta. EPA-600/9-91-026a.
Cothern, C. R., and P. A. Rebers, radon eds. 1990. *Radium and uranium in drinking water*. Michigan: Lewis Publication.

Cothern, C. R., and J. E. Smith, eds. 1987. *Environmental radon*. New York: Plenum Press.

Crameri, R., H. H. Brunner, R. Buchli, C. Wernli, and W. Burkart. 1989. Indoor Rn levels in different geological areas in Switzerland. *Health Physics* 57:29.

Cummings, J. B., J. J. Tooley, and N. Moyer. 1991. Investigation of air distribution system leakage and its impact on Central Florida houses. *Florida Solar Energy Center Report* FSEC-CR-397-91. Cocoa Beach, Florida.

Dyess T. M., T. Brennan, and M. Clarkin. 1993. Designs for new residential HAC systems to achieve radon and other soil gas reduction. Proceedings of the 1993 International Radon Conference, AARST, Denver.

Fejer, J. A. 1967. In *The encyclopedia of atmospheric sciences and astrogeology,* edited by R. W. Fairbridge. New York: Reinhold.

Fukuda, H. 1955. Air and vapor movement in soil due to wind gustiness. *Soil Sciences* 79:249.

Furrer, D., R. Crameri, and W. Burkart. 1991. Dynamics of Rn transport from the cellar to the living area in an unheated house. *Health Physics* 60: 393.

Garzon, L., J. M. Juanco, J. M. Perez, J. M. Fernandez, and B. Arganaz. 1986. The universal Rn wave: an approach. *Health Physics* 51:185.

Gumming, C., and A. G. Scott. 1982. Radon and thoron daughters in housing. *Health Physics* 42:527.

Hems, G. 1966. Acceptable concentration of radon in drinking water. *International Journal of Air and Water Pollution* 10:769.

Hubbard, L. M., B. Bolker, R. A. Socolow, D. Dickerboff, and R. B. Mosley. 1989. Radon dynamics in a house heated alternatively by forced air and by electric resistance. Proceedings of the 1988 Symposium on Radon and Radon Reduction Technology, Vol. 1, EPA-600/9-89-006a (NTIS PB89-167480).

Hull, D. A., and T. A. Reddy. 1990. Study on the reliability of short-term measurements to predict long-term basement radon levels in a resident. Proceedings of the 1990 International

Symposium on Radon and Radon Reduction Technology, Atlanta. EPA: EPA-600/9-91-026a.

James, A. C. 1984. Dosimetric approaches for risk assessment for indoor exposure to radon daughters. *Radiation Protection Dosimetry* 7:353.

Kahlos, H., and M. Asikainen. 1980. Internal radiation doses from radioactivity of drinking water in Finland. *Health Physics* 39:108.

Kozik, A. C., P. Oppenheim, and D. Schneider. 1993. The effect of interior door position and methods of handling return air on differential pressures in a Florida house. *The 1992 international symposium on radon and radon reduction technology* 1:79-92. EPA-600/R-93-083a. NTIS PB93-196194. Springfield, Va.

Landman, K. A. 1982. Diffusion of radon through cracks in a concrete slab. *Health Physics* 30:65.

Makofske, W. J., and M. R. Edelstein, eds. 1988. *Radon and the environment*. New Jersey: Noyes Publications.

National Academy of Science. 1988. *Health risks of radon and other internally deposited alpha-emitters*. BEIR IV. Washington, D.C.: National Academy of Science Press.

Nazaroff, W. W., A. Feustal, A. Nero, K. L. Revzan, D. T. Grimsrud, M. A. Essling, and R. E. Toohey. 1988. Radon transport into a detached one-story house with a basement. *Atmospheric Environment* 19:31.

Nazaroff, W. W., S. R. Lewis, S. M. Doyle, B. A. Moed, and A. V. Nero. 1987. Experiments on pollutant transport from soil into residential basements by pressure-driven airflow. *Environmental Science and Technology* 21:459.

Nazaroff, W. W., B. A. Moed, and R. G. Sextro. 1988. Soil as a source of indoor radon: generation, mitigation and entry. In *radon and its decay products in indoor air*, edited by W. W. Nazaroff and A. V. Nero. New York: John Wiley and Sons.

Nero, A. V. 1988. Radon and its decay product in indoor air: an overview. In *radon and its decay products in indoor air*, edited by W. W. Nazaroff and A. V. Nero. New York: John Wiley

and Sons.

Nero, A. V., and W. W. Nazaroff. 1984. Characterizing the source of radon indoors. *Radiation Protection Dosimetry* 4:23.

Nielson, K. K., and V. C. Rogers. 1991. Modeling indoor radon entry from soil radon emanation and transport. *Proceedings of the Radon Modeling Workshop of the Florida Radon Research Program*, edited by D. E. Hintenlang. EPA-AEERL, Research Triangle Park, N.C.

Owczarski, P. C., D. J. Holford, H. D. Freeman, and G. W. Gee. 1990. Effects of changing water content and atmospheric pressure on radon flux from surfaces of five soil types. *Geophysical Research Letters* 17, no. 6:817.

Prichard, H. M., and T. F. Gesell. 1981. An estimate of population exposure due to radon in public water supplies in the area of Houston, Texas. *Health Physics* 41:599.

Reddy, T. A., F. B. Molineaux, K. J. Gadsby, and R. H. Scocolow. 1990. Statistical analyses of radon levels in residences using weakly and daily averaged data. PU/CEES report no. 249.

Rogers, V. C., K. K. Nielson, and D. R. Kalkwarf. 1984. *Radon attenuation handbook for uranium mill tailings cover design*. Report NUREG/CR-3533, U.S. Nuclear Regulatory Commission.

Rogers, V. C., and K. K. Nielson. 1991. Multiphase radon generation and transport in porous materials. *Health Physics* 60:807.

Salimitari, E., F. T. Najafi, and K. K. Al-Ahmady. 1996. Experimental investigation of soil water content effects on in-situ soil-gas radon testing prior to construction. *Proceedings of the 1996 International Radon Symposium* II3.1-II3.7.

Scheidegger, A. E. 1960. *The Physics of Flow through Porous Media*, 2d ed. New York: John Wiley and Sons.

Schery, S. D. 1985. Measurements of airborne ^{212}Pb and ^{220}Rn concentrations at varied indoor locations within the united States. *Health Physics* 49:1061.

Smith, B. M., W. N. Grune, F. B. Higgins, and J. G. Terrill. 1961. Natural radiology in ground water supplies in Maine and

New Hampshire. *Journal of American Water Workers Association* 53:75.

Steck, D. J. 1990. A comparison of epa screening measurements and annual ^{222}Rn concentrations in statewide surveys. *Health Physics* 60:523.

Stranden, E. 1988. Building materials as a source of indoor radon. In *radon and its decay products in indoor air,* edited by W. W. Nazaroff and A. V. Nero. New York: John Wiley and Sons.

Stranden, E., A. K. Kolstad, and B. Lind. 1984. The influence of moisture and temperature on radon exhalation. *Radiation Protection Dosimetry* 7:55.

Strong, K. P., and D. M. Levins. 1982. Effect of moisture content on radon emanation from uranium ore and tailings. *Health Physics* 42:27.

Suomela, M., and H. Kahlos. 1972. Studies on the elimination rate and radiation exposure following ingestion of ^{222}Rn-rich water. *Health Physics* 23:641.

Tanner, A. B. 1964. Radon mitigation in the ground: A review. In *Natural radiation environment,* edited by J. A. Adams and W. M. Lowder. Chicago: University of Chicago Press.

Tanner, A. B. 1980. Radon migration in the ground: A supplementary review. *Proceedings of Natural Radiation Environment III,* edited by F. Gesell and W. M. Lowder. Conf. 780422, U.S. Department of Commerce. National Technical Information Service. Springfield, Va.

Toohey, R. E. 1987. Radon vs. lung cancer: New study weighs the risks. Argonne National Laboratory logos 5:7.

Toth, A. 1984. Simple field method for determining of ^{220}Rn and ^{222}Rn daughter energy concentrations in room air. *Radiation Protection Dosimetry* 7:247.

Turner, R. C., J. M. Radley, and W. V. Mayneord. 1961. Naturally occurring alpha-activity of drinking waters. *Nature* 189:348.

Tsang, Y. W., and T. N. Narasimhan. 1991. Effects of periodic atmospheric pressure variation on radon entry into buildings.

Journal of Geophysical Research 97:9161.

United Nations Scientific Committee on the Effect of Atomic Radiation. 1982. *Ionizing radiation: sources and biological effects.* New York: United Nations Press.

U.S. Department of Energy. 1986. *Understanding radiation.* Energy booklet DOE/NE-0074.

U.S. Department of the Interior. 1992. *The geology of radon.* U.S. Geological Survey. U.S. Government Printing Office 0-326-248.

U.S. Environmental Protection Agency. 1986. *A citizen's guide to radon, what it is and what to do about it.* U.S. Environmental Protection Agency and Department of Health and Human Services OPA-86-004.

U.S. Environmental Protection Agency. 1992. *A citizen's guide to radon.* 2d edition. U.S. Environmental Protection Agency, Air and Radiation ANR-464, 402-k92-001.

U.S. Environmental Protection Agency. 1988. *Application of radon reduction methods.* EPA/625/5-88/024. Air and Energy Engineering Research Laboratory, N.C.

BIOGRAPHICAL SKETCH

My name is Esfandiar Salimi Tari. I was born on November 3, 1954, in Tehran, Iran. I am the first child in a family of six children. I received my diploma in Tehran in 1974 and then was drafted into the military for two years. I first came to the United States in February 1977. I returned to my country in 1978 and got married. I came back to the United States with my wife, Pouran, and we both enrolled at California State University at Sacramento. I received my bachelor's degree in mechanical engineering from California State University at Sacramento in 1983. I received my master's degree in irrigation engineering at Utah State University at Logan in 1988. My wife and I moved to Gainesville, Florida, and I applied for a Ph.D. in civil engineering at the University of Florida. I worked with Dr. Najafi on various research projects before becoming involved with radon research. This research interested me, and I decided to write my dissertation on it. My wife and I had a daughter, Maryam, in 1992. Besides going to school full time, I also run my own business.

I certify that I have read this study and that in my opinion it conforms to acceptable standards of scholarly presentation and is fully adequate, in scope and quality, as a dissertation for the degree of Doctor of Philosophy.

Fazil T. Najafi, Chairman
Associate Professor of
Civil Engineering

I certify that I have read this study and that in my opinion it conforms to acceptable standards of scholarly presentation and is fully adequate, in scope and quality, as a dissertation for the degree of Doctor of Philosophy.

Mang Tia
Professor of Civil
Engineering

I certify that I have read this study and that in my opinion it conforms to acceptable standards of scholarly presentation and is fully adequate, in scope and quality, as a dissertation for the degree of Doctor of Philosophy.

Samim Anghaie
Professor of Nuclear and
Radiological Engineering

I certify that I have read this study and that in my opinion it conforms to acceptable standards of scholarly presentation and is fully adequate, in scope and quality, as a dissertation for the degree of Doctor of Philosophy.

Roy J. Bolduc
Professor Emeritus
of Instruction and
Curriculum

I certify that I have read this study and that in my opinion it conforms to acceptable standards of scholarly presentation and is fully adequate, in scope and quality, as a dissertation for the degree of Doctor of Philosophy.

Kaiss Al-Ahmady
Consultant of Conley,
Rose, Tayon, PC
Austin, Tx

This dissertation was submitted to the Graduate Faculty of the College of Engineering and to the Graduate School and was accepted as partial fulfillment of the requirements for the degree of Doctor of Philosophy.

May, 1999

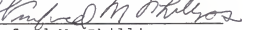

Winfred M. Phillips
Dean, College of
Engineering

M. J. Ohanian
Dean, Graduate School